A reference transcriptome for the early-branching fern *Botrychium lunaria* enables fine-grained resolution of population structure

Vinciane Mossion[1], Benjamin Dauphin[1,2], Jason Grant[1], Niklaus Zemp[3], Daniel Croll[1 *]

[1] Laboratory of Evolutionary Genetics, University of Neuchâtel, Neuchâtel, Switzerland
[2] WSL Swiss Federal Research Institute, Birmensdorf, Switzerland
[3] Genetic Diversity Centre (GDC), ETH Zurich, Zurich, Switzerland
[*] Corresponding author: daniel.croll@unine.ch

Data availability: Raw sequencing reads and the assembled transcriptome are available at the NCBI Short Read Archive under the Bioproject accession PRJNA605155.

Author contributions: VM, BD and DC designed the study. VM and DC performed analyses, NZ contributed analyses tools, BD and JG acquired funding. VM and DC wrote the manuscript with input from the others.

Running title: A reference transcriptome for *Botrychium lunaria*

Abstract

Ferns are the second most dominant group of land plants after angiosperms. Extant species occupy an extensive range of habitats and contribute significantly to ecosystem functioning. Despite the importance of ferns, most taxa are poorly covered by genomic resources. The genus *Botrychium* belongs to one of the earliest divergent lineages of vascular plants and has a global distribution with 35 species, half of which are polyploids. Here, we establish a reference transcriptome for *Botrychium lunaria*, a diploid species with an extremely large genome of 27.5 Gbp. We assembled 25,721 high-quality transcripts with an average length of 1,332 bp based on deep RNA-sequencing of a single individual. We sequenced an additional 11 transcriptomes of individuals from two populations in Switzerland, including the population of the reference individual. Based on read mapping to reference transcript sequences, we identified 374,510 single nucleotide polymorphisms (SNPs) segregating among individuals for an average density of 14 SNPs per kb. The transcriptome-wide markers provided unprecedented resolution of the population genetic structure revealing substantial variation in heterozygosity among individuals. We also constructed a phylogenomic tree of 73 taxa representating all fern orders to ascertain the placement of the genus *Botrychium*. The high-quality transcriptomic resources enable powerful population and phylogenomic studies in an important group of ferns.

Significance statement

Ferns pose substantial puzzles in terms of lifestyles, genome organization and population structure. Progress has been significantly hampered by the lack of genomic resources. Here, we present a reference transcriptome for *Botrychium lunaria*, a phylogenetically early-branching fern with an extremely large genome of 27.5 Gbp. We show that the new transcriptome improves phylogenetic resolution among early-branching ferns. Based on an additional 11 transcriptomes of the same species, we identify unexpected variation in population-level heterozygosity.

Introduction

Ferns (Polypodiopsida) constitute the oldest lineage of vascular plants along with lycophytes (Lycopodiopsida) (Kranz and Huss, 1996; Kenrick and Crane, 1997; PPG I, 2016). With 85% of the total species richness found in the tropics, ferns are present in most climates (Page, 2002; Ranker and Haufler, 2008). Habitats of ferns include deserts, grasslands, forest understory, mountainous regions, and aquatic environments (Klaus *et al.*, 2010) where they have diversified into a multitude of lifestyles. Ferns play key roles in ecosystem functioning including serving as a habitat for invertebrates (Ellwood and Foster, 2004), shaping plant recolonization of disturbed habitats (Walker, 1994) and influencing the tree species communities composition (George and Bazzaz, 1999a; George and Bazzaz, 1999b). Ferns have complex and idiosyncratic life cycles characterized by the growth of gametophytes dependent on endosymbiotic fungi. In contrast to other plants, many fern species are capable of versatile reproductive modes (Sessa *et al.*, 2012) including apomixes, sporophytic and gametophytic selfing, as well as outcrossing (Barker and Wolf, 2010; Haufler *et al.*, 2016). Yet, our understanding of the evolutionary origins and lifestyle diversification is limited.

Phylogenetic analyses resolved the position of ferns as the sister group to seed plants (Pryer *et al.*, 2001) and as the second earliest diverging lineage of vascular land plants (Raubeson and Jansen, 1992; Pryer *et al.*, 2004). The age of the fern clade was estimated to be ca. 364-420 million years underlining the deep divergence among ferns lineages (Pryer *et al.*, 2004; Schuettpelz and Pryer, 2007; Rai and Graham, 2010; Knie *et al.*, 2015). Fern phylogenies have been mainly established based on chloroplast markers (Schuettpelz and Pryer, 2007; Rai and Graham, 2010; Testo and Sundue, 2016) in combination with ribosomal (Pryer *et al.*, 2001; Pryer *et al.*, 2004) and mitochondrial markers (Knie *et al.*, 2015). However, plastid and mitochondrial markers often failed to resolve within-genus level differentiation and events of reticulate evolution. A further challenge to resolve fern phylogenies is that almost a third of speciation events were driven by polyploidization (Wood *et al.*, 2009). Hence, genome- or transcriptome-wide datasets are needed to accurately resolve the evolutionary relationships.

The first insights into the structure of fern genomes were provided by two complete genome sequences of *Azolla filiculoides* and *Salvinia cucullata* (Li *et al.*, 2018). These two species belong to the 1% heterosporous fern species in contrast to the dominant homosporous species. Heterosporous ferns exhibit the smallest known genomes as shown for the closely related species *A. microphylla* and *S. molesta* (0.77 Gbp and 2.28 Gbp, respectively; Obermayer *et al.*, 2002; Clark *et al.*, 2016). Conversely, homosporous fern genomes contain on average three times more chromosomes than heterosporous ferns and seeds plants (Barker and Wolf 2010). The recent release of a partial genome assembly for the heterosporous fern *Ceratopetris richardii* highlighted the challenge associated with

complex fern genomes (Marchant *et al.*, 2019). In contrast, a series of recent phylogenomic studies highlighted the power of transcriptome-based approaches (Wickett *et al.*, 2014; Shen *et al.*, 2017; Leebens-Mack *et al.*, 2019).

Major progress in the establishment of genomic resources was made with the sequencing of 74 fern transcriptomes (Matasci *et al.*, 2014; Leebens-Mack *et al.*, 2019). Such datasets were successfully used to develop single copy nuclear markers to resolve deep evolutionary relationships among ferns (Rothfels *et al.*, 2013; Rothfels *et al.*, 2015). In addition, transcriptomes can be used to develop genotyping approaches to overcome challenges associated with large genome sizes in non-model organisms. These approaches typically reduce genome complexity but still provide sufficient polymorphic markers to conduct population genomics analyses (Seeb *et al.*, 2011). Major methods include exome capture (Yeaman *et al.*, 2016), RNA-sequencing (Sloan *et al.*, 2012), double-digest restriction-site associated DNA sequencing (Peterson *et al.*, 2012), and targeted re-sequencing (Rellstab *et al.*, 2016). Establishing and expanding transcriptomic datasets for understudied fern clades will bring about major new insights into fern diversification.

An important genus lacking transcriptomic resources is *Botrychium* belonging to the second most early-branching fern subclass, the Ophioglossidae (PPG I, 2016). This subclass is characterized by a subterranean gametophytic stage (Jeffrey, 1898; Winther and Friedman, 2007; Field *et al.*, 2015) and extremely large and complex genomes (e.g. *Ophioglossum reticulatum* n=720 chromosomes) (Khandelwal, 1990). *Botrychium* occurs in open habitats on nearly every continent across a broad temperate and boreal distribution. This genus is divided into three monophyletic clades defined by maternally inherited markers (Simplex-Campestre, Lanceolatum and Lunaria) (Dauphin *et al.*, 2017), containing 35 recognized taxa (PPG I, 2016). The challenge of identifying *Botrychium* taxa based on morphology is underlined by claims of cryptic species (Clausen, 1938; Hauk, 1995). Ambiguous morphologies are sometimes caused by polyploidization which is a major driver of speciation as half of the known *Botrychium* species are allopolyploids (Dauphin *et al.*, 2018). Nuclear markers resolved the parental origins of these allopolyploid taxa and provided insights into the genus radiation approximately 2 million years ago. Additional, the reconstruction of maternal lineages of *Botrychium* revealed genetic diversity within the Lunaria clade highlighting the uncertainty of taxonomic assignments (Dauphin *et al.*, 2014; Dauphin *et al.*, 2017). Previous population genetic studies based on isozymes showed a lack of genetic differentiation among morphologically recognized types (Williams *et al.*, 2016). Poor resolution between *Botrychium* populations suggests pervasive self-fertilization (Farrar, 1998; Hauk and Haufler, 1999). Genetic studies suggest that cross-fertilization may be relatively frequent (Camacho and Liston, 2001; Swartz and Brunsfeld, 2002; Birkeland *et al.*, 2017). However, the life histories of these early-branching ferns remain largely unresolved due to the lack of genome-wide markers.

In this study, we assemble and curate the transcriptome of *B. lunaria* with a massive genome size of 27.5 Gbp (Dauphin *et al.*, 2016) filling an important gap in the fern phylogeny. By analyzing the transcriptome of an additional 11 individuals, we show that individuals vary substantially in terms of genotype and heterozygosity within and between populations. We further demonstrate the power of transcriptome-wide markers to resolve phylogenetic relationships at the genus level and among deeply divergent fern lineages.

Material and Methods

Sampling, library preparation and sequencing

Leaf material of *B. lunaria* was obtained from three locations in Switzerland: two in the Valais Alps in Val d'Hérens, Mase and Forclaz within approximately. 30 km, and one in the Jura Mountains at Chasseral (Suppl. Table S1). Leaves of six individuals from Val d'Hérens and from Chasseral were collected in July 2015 and June 2017, respectively. Plant material was wrapped in aluminum foil and frozen immediately in liquid nitrogen. Total RNA was extracted from trophophores (i.e. sterile part of leaves) using the RNAeasy Plant Mini Kit (Qiagen) and DNA was eliminated using DNase I digestion. Total RNA was quantified using a Qubit fluorometer (Invitrogen, Thermo Fisher Scientific) with the RNA Broad-Range assay kit (Invitrogen, Thermo Fisher Scientific) and quality-checked using an Agilent 2200 Tape Station (AgilentTechnologies, Inc.). Samples were diluted to 100 ng/µl in RNase free ultra-pure water before library preparation. The RNA-sequencing libraries were prepared following a TruSeq RNA library preparation protocol (Illumina, Inc.) enriching for polyadenylated RNAs. After quality assessment on an Agilent 2200 Tape Station, libraries were pooled and sequenced in 150 bp single-end mode on one lane of an Illumina HiSeq 4000 sequencer.

De novo assembly, filtering and quality assessment

Sequencing reads were quality-checked using FastQC v. 0.11.7 (Andrews, 2010) and trimmed using Trimmomatic v. 0.38 (Bolger *et al.*, 2014). Reads were retained if the leading and trailing bases > 5, a 4-bp sliding window > 15, and a minimum read length of 36 bp. Trimmed transcript sequences were then *de novo* assembled using Trinity v. 2.8.3 (Haas *et al.*, 2013) from a single reference individual). We used the pseudo-alignment percentage calculated by Kallisto v. 0.45.0 (Bray *et al.*, 2016) to assess the representativeness of the raw assembly across the twelve sequenced individuals in total. Candidate coding regions were identified using TransDecoder v. 5.3.0 (Haas *et al.*, 2013). Only transcripts with an open reading frame (ORF) of at least 100 amino acids were kept. We also retained only the longest isoform per transcript using the Trinity v. 2.8.3 toolkit. We used Diamond v. 0.9.24 (Buchfink *et al.*,

2015) to screen the transcript assembly against the NCBI non-redundant protein database (nr) to identify potential foreign RNA contaminants. The best hit for each transcript was assigned at the phylum-level using the R package *taxise* v. 0.9.7 (Chamberlain and Szöcs, 2013) in RStudio v.1.2.1335 (RStudio Team, 2015; R Development Core Team, 2020). We excluded all transcripts with a best hit outside of the plant kingdom. The completeness of the transcriptome assembly was assessed using BUSCO v. 3 with the embryophyta_odb10 database (Simão *et al.*, 2015). Data were visualized using the R package *ggplot2* v. 3.1.0 (Wickham, 2016).

Variant calling

We generated alignment BAM files for each individual against the reference transcriptome using the short read aligner Bowtie2 v. 2.3.5 (Langmead, 2010) and SAMtools v. 1.9 (Li *et al.*, 2009). Depth coverage of the reference individual was extracted using SAMtools idxstats. Alignments were processed with HaplotypeCaller implemented in the Genome Analysis Toolkit (GATK) v. 4.1.0.0 (DePristo *et al.*, 2011; McKenna *et al.*, 2010; Van der Auwera *et al.*, 2013) for single nucleotide polymorphism (SNP) calling. The resulting gvcf files were combined and genotyped using the GATK CombineGVCF and GenotypeGVCF tools, respectively. We excluded monomorphic sites from further analysis. We filtered SNPs for the number of genotyped chromosomes (AN $\geq$ 20) out of a maximum of 24 (12 diploid individuals). Quality criteria QUAL > 100, QualByDepth > 5.0, RMSMappingQuality > 20.0, MappingQualityRankSumTest retained values > -2.0 and < 2.0, and ReadPosRankSumTest and BaseQualityRankSumTest retained values > -2.0 and < 2.0 were defined following the best practices and were applied to flag low-quality loci (Suppl. Figure S1). We removed SNPs failing the above filters using VCFtools v. 0.1.16 (Danecek *et al.*, 2011) and added a filter to retain only bi-allelic SNPs. These analyses were performed using the R packages *vcfR* v. 1.8.0 (Knaus and Grünwald, 2017) and the SNP statistics among transcripts were visualized using *ggplot2* v. 3.1.0.

Population genetics analyses

To avoid biases introduced by highly polymorphic transcripts and to reduce the computational time of population genetic analysis, we subsampled the number of SNPs by selecting one SNP every 1,000 bp of transcriptomic sequence using VCFtools v. 0.1.16. We performed principal component analyses (PCA) and calculated the pairwise F_{ST} and the mean heterozygosity (H_e) per location and per individual. These analyses were performed using the R packages *vcfR* v. 1.8.0, *adegenet* v. 2.1.1 (Jombart and Ahmed, 2011) and *hierfstat* v. 0.04-22 (Goudet, 2005) and data were visualized using *ggplot2* v. 3.1.0.

Functional annotation

We functionally characterized encoded protein sequences based on gene ontology (GO) terms. We summarized GO terms by selecting the least redundant annotations among the 30 most frequent terms per ontology (cellular component CC, molecular function MF, and biological process BP). Analyses were performed using the Bioconductor packages *AnnotationDbi* v. 1.46.0 (Pagès *et al.*, 2020), *GO.db* v. 3.8.2 (Carlson, 2020), *GSEABase* v. 1.34.0 (Morgan *et al.*, 2020), *annotate* v. 1.62.0 (Gentleman, 2020), and data were visualized using the R packages *ggplot2* v. 3.1.0.

Genus-level phylogenetic analyses

We analysed published sequences of four nuclear regions from diploid and polyploid *Botrychium* taxa: *ApPEFP_C*, *CRY2cA*, *CRY2cB*, and *transducin* (Dauphin *et al.*, 2018). We searched homologous sequences in the transcriptome assembly using BLAST v. 2.9.0 (Altschul *et al.*, 1990). If the associated transcript was found in the assembly, we used BCFtools v. 1.9 (Li, 2011) to retrieve the corresponding transcript from the 11 remaining individuals using the VCF file information. Sequence alignments were performed using MAFFT v. 7.407 using the L-INS-i strategy and default parameters (Katoh *et al.*, 2002; Katoh and Standley, 2013). Multiple alignments were visually inspected and cleaned by removing any potentially misaligned segments using Geneious v. 8.1.9 (Kearse *et al.*, 2012). Phylogenetic trees were inferred using maximum likelihood (ML) in RAxML-NG v. 0.9.0 (Kozlov *et al.*, 2019). We ran tree inferences with a fixed random seed of 2 under the HKY+GAMMA model based on model settings by Dauphin *et al.* (2018) to ensure reproducibility. The tree search was performed using 25 random- and 25 parsimony-based starting trees. The branch support was estimated using 1,000 bootstrap replicates and then depicted on the best-scoring ML tree. Final gene trees were edited with FigTree v. 1.4.4 (Rambaud, 2009).

Phylogenomic analyses

We performed phylogenomic analyses across ferns by including the newly established *B. lunaria* transcriptome and 79 additional transcriptomes, including 73 fern species (10 Eusporangiates, 63 Leptosporangiates), and 5 outgroups (Lycopodiopsida) (Suppl. Table S2) (Leebens-Mack *et al.*, 2019). We first performed an ortholog search using OrthoFinder v. 2.3.3 (Emms and Kelly, 2015) including the newly established *B. lunaria* transcriptome and protein sequences of the 1000 Plants Project. We retained only orthogroups with members found in at least 67 species (>90% of total), with a minimum of 59 species (>80%) carrying a single copy of the orthogroup. Species represented in less than 50% of the orthogroups were removed from the dataset. Then, we randomly selected one orthologous copy for each remaining species having multiple gene copies. Sequences of the orthogroups subset were subsequently aligned with MAFFT v. 7.407 under the L-INS-i strategy and default parameters. The optimal substitution model was assessed for each orthogroup gene using the AIC- and BIC-based model test implemented in RAxML-NG v. 0.9.0. Finally, gene trees were built using maximum

likelihood (ML) in RAxML-NG v. 0.9.0. We ran tree inferences under the LG4M (Le and Gascuel, 2008) model with a fixed random seed of 2. The tree search was performed on 25 random and 25 parsimony-based starting trees and branch support was estimated over 100 bootstrap replicates. The inferred gene trees were used to estimate a species tree with Astral v. 5.5.6 (Mirarab *et al.*, 2014; Zhang *et al.*, 2018). Branch support was calculated using multi-locus bootstrapping (Seo, 2008) and local posterior probabilities (Sayyari and Mirarab, 2016). The species tree was edited with FigTree v. 1.4.4 (Rambaud, 2009).

Results

Sample collection and reference transcriptome assembly

In total, twelve *B. lunaria* individuals were sampled from Val d'Hérens and Chasseral located in the Valais Alps and the Jura Mountains, respectively. The two sites are approximately 120 km apart and the alpine population was sampled on meadows on an altitudinal range of 1,500 to 2,400 meters (Suppl. Table S1). The transcriptome sequencing produced 14.6-50.1 million reads per individual. After quality trimming, we retained 97.0-99.2% of the reads (Figure 1A, Suppl. Table S3). The highest number of high-quality reads (49.5 million) were obtained for the Chasseral individual CHA_I_1. Hence, we selected this individual to produce a reference transcriptome. The raw assembly for the reference individual (CHA_I_1) contained 167,306 transcripts for a total of 87,537 candidate genes. Mapping reads from individuals to the raw transcriptome assembly showed an alignment rate between 74.2-82.5% regardless of the population of origin (Figure 1A, Suppl. Table S3). We analyzed all transcripts for the presence of high-confidence open reading frames (ORF; ≥100 amino acids). We retained 69,280 transcripts (41.4%) covering 26,139 predicted genes (Figure 1B). Next, we selected the longest transcript for each gene (Figure 1D). We performed a screen of each gene against the complete non-redundant protein database of NCBI and found evidence for contamination in 418 transcripts. Most contaminant sequences were associated with viruses, fungi and bacteria (Figure 1C). The final assembly consisted of 25,721 unique transcripts spanning a total of 34.25 Mb. The average and median transcript length were 1,332 and 965 bp, respectively (Figure 1D). The N50 of the final transcriptome was 1,995 bp with an average GC content of 44.3% (Figure Table 1). GO terms were assigned to 12,154 (47.2%) transcripts (Figure 2).

Completeness of the B. lunaria transcriptome

We assessed the completeness of the assembled *B. lunaria* reference transcriptome using BUSCO. Importantly, none of the 30 species constituting the BUSCO embryophyta_odb10 database belongs to

ferns *lato sensu*. We found 73.9% complete single-copy, 1.4% complete duplicates, 12% fragmented and 12.7% missing genes for the *B. lunaria* transcriptome (Figure 1E, Table 2). This is comparable to the only two complete genome assemblies of ferns that include *A. filiculoides* with 72.5% complete single-copy and *S. cucullata* with 79.7% complete single-copy (Figure 1E, Table 2). The two Salviniaceae genomes and the *B. lunaria* transcriptome exhibited a comparable number of missing BUSCO genes (12.5%, 13.7% and 12.6%, respectively; Figure 1E, Table 2). The *B. lunaria* transcriptome showed a higher percentage of fragmented BUSCO genes compared to genome assemblies of *A. filiculoides* and *S. cucullata*, (12.0%, 5.6% and 2.5%, respectively; Figure 1E, Table 2). The mapped reads coverage depth of the reference individual to the assembled transcripts is on average 1,648 with a range of 4 to 514,622. Most of the transcripts exhibited a moderate coverage (Figure 3A) whereas few (6.9%) showed a coverage > 4004. The read coverage increased with transcript length (Figure 3B).

Identification of within-species transcriptomic polymorphism

We mapped reads from the twelve sequenced transcriptomes to the newly established reference transcriptome to identify segregating variants within the species (Figure 3C). The mapping rate of each individual varied between 82.1-86.7%. We found no meaningful difference in mapping rates among populations and individuals. The highest mapping rate was found for the individual IIT1_H5 (86.7%), which was slightly higher than the mapping rate of the reference individual used to establish the transcriptome (CHA_I_1, 85.5%; Suppl. Table S3). Based on reads aligned against reference transcripts, we called SNPs and genotyped each individual as a diploid. We recovered a total of 374,510 high-quality bi-allelic SNPs after filtering. The average number of SNPs per transcript was 17 and the maximum number was 249 (Figure 4A). The SNP density per transcript had a mean of 14, a median of 10.2, and a maximum of 160 SNPs per kb (Figure 4B). The mean and median SNP density increased with transcript length (Figure 4C).

Population structure and heterozygosity

We used the SNP genotyping data from the twelve individuals to assess the degree of population differentiation between the sampling locations (Figure 5A). The first principal component (PC1, 17%) of the principal component analysis (PCA) identified a divergent genotype in the Chasseral population (CHA_I_7, Figure 5B). The second principal component (PC2, 12%) separated the two populations Chasseral and Val d'Hérens (Figure 5B). We performed a second PCA excluding the CHA_I_7 individual and found the Chasseral population to be more diverse than Val d'Hérens (Figure 5C). We found no apparent differentiation between the two locations sampled in Val d'Hérens (Forclaz and Mase) and the pairwise F_{ST} (0.079) was low. The mean heterozygosity was slightly higher in Val d'Hérens (0.20) than in the Chasseral population (0.17; Figure 5D). We found similar levels of

variation in individual heterozygosity among populations ranging from 0.16 to 0.21, except for CHA_I_7, which was an outlier on the PCA (Figure 5E). CHA_I_7 showed less than half the heterozygosity (0.05) compared to other members of the same population.

Phylogenetic inference among Botrychium species

We analyzed available multi-locus sequence data to place the twelve individuals analyzed at the transcriptome level. Among the four nuclear loci previously sequenced in a broad sample of *Botrychium* species, three loci are known to display sequence variation nearly exclusively in intronic sequences (Dauphin *et al.*, 2018). Hence, no comparisons with our transcriptomic sequences were possible. We focused on the locus CRY2cA carrying enough informative sites in the coding regions to produce a well-supported phylogeny. The combined dataset for CRY2cA included 67 individuals representing 38 *Botrychium* taxa and 2 outgroups (Dauphin *et al.*, 2018) (Suppl. Table S4). The multiple sequence alignment contained a total of 812 sites, of which 64 were variable. The main clades Lanceolatum, Lunaria, and Simplex-Campestre were resolved as being monophyletic (Figure 6). Lanceolatum and Simplex-Campestre were resolved as sister groups. All individuals from the Chasseral and Val d'Hérens grouped with *B. lunaria* var. *lunaria* and formed a well-supported clade.

Transcriptome-wide phylogenomic tree of ferns

We retrieved complete transcriptomes of 78 species covering the phylogenetic breadth of ferns (Leebens-Mack *et al.*, 2019) in order to robustly place the *B. lunaria* transcriptome. We identified 13,358 orthogroups in total of which we retained 864 orthogroups and 74 species to construct a phylogenomic tree. The species tree topology was congruent with recent fern phylogenies (PPG I, 2016; Shen *et al.*, 2017; Leebens-Mack *et al.*, 2019). We identified Equisetales as the sister clade to all other ferns and Marattiales as the sister clade to Psilotales and Ophioglossales. The *B. lunaria* transcriptome clustered with the sister genus *Sceptridium* and the closely related genus *Botrypus*. The species tree nodes were well supported both by the multi-locus bootstrap and the local posterior probabilities. However, the relationship between Hymenophyllales and Gleichenales was ambiguous and we found similar support for sister species and alternative scenarios. Similarly, the relationship between Salviniales and Cyatheales differed between the local posterior probability and multi-locus bootstrap trees. We found equal support for Cyatheales or Salviniales, respectively, being the sister group to Polypodiales (Figure 7, Suppl. Figure S2).

Discussion

We established a high-quality transcriptome for the genus *Botrychium* filling an important gap in the coverage of early-branching ferns. The completeness of the transcriptomic gene space was comparable to well-assembled fern genomes. Using twelve individuals of the same species sampled in two locations, we were able to generate the first dense SNP dataset for *B. lunaria* and early-branching ferns in general. We were also able to anchor the sequenced individuals in the phylogeny of other *Botrychium* species using a nuclear locus. A phylogenomic tree based on 864 orthologous genes confirmed the phylogenetic position of the genus among other ferns.

Establishment of a reference transcriptome for the Botrychium genus

Generating a representative transcriptome assembly is challenging because not all genes are expressed in all tissues and life cycle stages. Across the life cycle of ferns gene expression patterns are largely overlapping (Sigel *et al.*, 2018), but the covered gene space is usually increased by including multiple target tissues. For *Botrychium*, only the trophophore was an adequate candidate for the extraction of RNA since underground tissues are colonized by arbuscular mycorrhizal fungi (AMF) leading to numerous contaminants. In contrast, the sporophore carries spores and each spore contains an individual progeny genotype. Despite these challenges, our *B. lunaria* transcriptome has a fairly complete gene space in comparison to a wide range of assembled transcriptomes (Der *et al.*, 2011; Leebens-Mack *et al.*, 2019). It is important to note that database-dependent tools such as BUSCO consistently underestimate transcriptome completeness if the database was compiled without closely related species. The challenge in using BUSCO is exemplified by the absence of the earliest divergent vascular plants in the embryophyta dataset. The gene space of assembled fern genomes tends to show slightly less fragmented BUSCO genes compared to the *B. lunaria* transcriptome (Li *et al.*, 2018). However, the *B. lunaria* transcriptome is consistent with other high-quality fern transcriptomes (Leebens-Mack *et al.*, 2019). Missing gene segments in assembled transcriptomes are often caused by uneven read depth among genes or alternative splicing complicating gene recovery. The completeness of the *B. lunaria* transcriptome compared to other fern genomes and transcriptomes provides a powerful tool for phylogenetic and population analyses.

Fine-grained resolution of population structure

The transcriptome-wide SNPs revealed clear population structure between two *B. lunaria* populations sampled from Switzerland. The differentiation was apparent even when subsampling SNPs to contain a maximum of 1 SNP per kb to avoid biases by highly polymorphic transcripts. It was generally assumed *Botrychium* species populations show no genetic differentiation (Farrar, 1998; Hauk and Haufler, 1999) or low genetic differentiation (Camacho and Liston, 2001; Swartz and Brunsfeld, 2002; Birkeland *et al.*, 2017). The failure to resolve population differentiation in previous studies may well stem from the low resolution of allozyme markers. The transcriptome-wide markers showed every individual was clearly distinct, and populations showed marked differentiation. The Chasseral and Val

d'Hérens populations were collected in the Jura Mountains and Valais Alps, respectively. The two sites are 120 km apart and separated by habitats unsuitable for *B. lunaria*. Hence, reduced gene flow and genetic differentiation among populations is expected. We found no indication of genetic substructure among the two locations Mase and Forclaz within the Val d'Hérens valley. This suggests sufficient gene flow at the local scale or recent recolonization at the upper front of the valley, which is consistent with restriction-site associated DNA sequencing-based analyses of the same field sites (Dauphin, 2017).

Population-level genetic diversity is indicative of the reproductive mode of *Botrychium* species populations. Self-fertilization is common and includes sporophytic and gametophytic selfing. In sporophytic selfing, zygotes are produced by gametes from two distinct gametophytes but originate from a single sporophyte. In contrast, in gametophytic selfing, zygotes are produced from gametes of the same gametophyte. Gametophytic selfing is thought to be the main reproductive mode for the *Botrychium* genus and can lead to completely homozygous plants in one generation (Haufler *et al.*, 2016). In a population undergoing largely gametophytic selfing, very low genetic variation would be expected among individuals. Hence, the unique genotypes found in the Chasseral and Val d'Hérens populations suggest populations undergo either sporophytic selfing or outcrossing. Interestingly, one of the six Chasseral individuals exhibited less than half the heterozygosity observed in other individuals indicative of recent gametophytic selfing. The genetic diversity of *B. lunaria* populations and the clear structure among sites suggest that sporophytic selfing or outcrossing was dominant with a likely recent gametophytic selfing event. These findings contrast with the general assumption that gametophytic selfing is the dominant reproductive mode in the genus.

A refined phylogenetic placement of the Botrychium genus

The *B. lunaria* transcriptome enables strong phylogenetic inference at different taxonomic levels overcoming challenges associated with the small number of nuclear and chloroplast markers. *Botrychium* taxa cannot be easily delineated by morphological characteristics, hence taxonomy relies largely on phylogenetics (Dauphin *et al.*, 2014; Maccagni *et al.*, 2017; Dauphin *et al.*, 2017). We have placed the individual *B. lunaria* transcriptomes among other closely related taxa by retrieving orthologous genes, which were previously used for phylogenetic analyses. Despite challenges of low polymorphism in coding sequences of the loci, we were able to recapitulate the phylogenetic position of the reference individual used for transcriptome assembly and the 11 other *B. lunaria*. The newly established transcriptome will enable powerful genome-wide studies across the *Botrychium* genus. Importantly, markers developed using the transcriptome assembly will help to retrace the evolution of the extensive ploidy variation among *Botrychium*.

As an expansion of the phylogenetic analyses within *Botrychium*, we analyzed orthologous genes across all ferns and lycopods. The genus *Botrychium* was placed within the Ophioglossales with strong support. Furthermore, the phylogenomic tree supports the placement of the Marattiidae as a sister clade of the Ophioglossidae, which is consistent with Shen *et al.* (2017). The position of Marattiidae among the early divergent ferns remains poorly resolved. Leebens-Mack *et al.* (2019) showed an equal probability for Marattiidae being a sister clade to Psilotales and Ophioglossales and being a sister clade to the leptosporangiate ferns. Given that we largely based our phylogenomic tree on transcriptomes published by Leebens-Mack *et al.* (2019), the Marattiidae placement as a sister group to the Ophioglossidae is unexpected. A possible explanation for this difference is the addition of the *B. lunaria* transcriptome. The *Botrychium* genus constitutes one of the earliest diverging ferns and may improve the resolution of basal nodes.

Our study establishes a high-quality transcriptome for the early diverging fern genus *Botrychium.* With genome sizes estimated at 27.5 Gbp for *B. lunaria* (Dauphin *et al.*, 2016), the assembly of transcriptomes provides the only currently feasible approach to generate extensive genome-wide marker information. The transcriptomic markers will be powerful tools to investigate mating systems of ferns and polyploidization events. Furthermore, the transcriptome enables fine-grained demographic history analyses helping to dissect evidence for local adaptation across the diverse habitats of ferns.

Acknowledgements

We thank Frederic Sandoz for assistance in the field work. We thank Aria Minder and Sylvia Kobel for for input on laboratory methods. We acknowledge the 1KP sequencing consortium for advance access to transcriptomic sequences. Emilie Chanclud and Ursula Oggenfuss provided advice on bioinformatics. Ursula Oggenfuss, Leen N. Abraham, Simone Fouché, Pierre-Emmanuel Du Pasquier, Rose-Angela Ston and Giacomo Zilio provided helpful comments on a previous manuscript version. Data produced and analysed in this paper were generated in collaboration with the Genetic Diversity Centre (GDC), ETH Zurich and the Functional Genomics Center (FGC), Zurich. This work was supported by the Overhead fund of the University of Neuchâtel.

References

Altschul, S.F., Gish, W., Miller, W., Myers, E.W. and Lipman, D.J. (1990) Basic local alignment search tool. *J. Mol. Biol.*, **215**, 403–410.

Andrews, S. (2010) FastQC A Quality Control tool for High Throughput Sequence Data. Available at: http://www.bioinformatics.babraham.ac.uk/projects/fastqc/ [Accessed August 30, 2019].

Barker, M.S. and Wolf, P.G. (2010) Unfurling Fern Biology in the Genomics Age. *BioScience*, **60**, 177–185.

Birkeland, S., Borgenkjetne, I., Brysting, A.K., Elven, R. and Alsos, I.G. (2017) Living on the edge: Conservation Genetics of Seven Thermophilous Plant Species in a High Arctic Archipelago. *AoB PLANTS*, **9**.

Bolger, A.M., Lohse, M. and Usadel, B. (2014) Trimmomatic: a flexible trimmer for Illumina sequence data. *Bioinformatics*, **30**, 2114–2120.

Bray, N.L., Pimentel, H., Melsted, P. and Pachter, L. (2016) Near-optimal probabilistic RNA-seq quantification. *Nat. Biotechnol.*, **34**, 525–527.

Buchfink, B., Xie, C. and Huson, D.H. (2015) Fast and sensitive protein alignment using DIAMOND. *Nat. Methods*, **12**, 59–60.

Camacho, F.J. and Liston, A. (2001) Population structure and genetic diversity of Botrychium pumicola (Ophioglossaceae) based on inter-simple sequence repeats (ISSR). *Am. J. Bot.*, **88**, 1065–1070.

Cao, J., Schneeberger, K., Ossowski, S., et al. (2011) Whole-genome sequencing of multiple Arabidopsis thaliana populations. *Nat. Genet.*, **43**, 956–963.

Carlson, M. (2020) *GO.db: A set of annotation maps describing the entire Gene Ontology*, Bioconductor version: Release (3.10). Available at: https://bioconductor.org/packages/GO.db/.

Chamberlain, S.A. and Szöcs, E. (2013) taxize: taxonomic search and retrieval in R. *F1000Research*, **2**, 191.

Clark, J., Hidalgo, O., Pellicer, J., et al. (2016) Genome evolution of ferns: evidence for relative stasis of genome size across the fern phylogeny. *New Phytol.*, **210**, 1072–1082.

Clausen, R.T. (1938) A Monograph of the Ophioglossaceae. *Mem. Torrey Bot. Club*, **19**, 1–177.

Danecek, P., Auton, A., Abecasis, G., et al. (2011) The variant call format and VCFtools. *Bioinformatics*, **27**, 2156–2158.

Dauphin, B. (2017) *Evolution of moonwort ferns ("Botrychium", Ophioglossaceae) on local to global scales*. University of Neuchâtel.

Dauphin, B., Farrar, D.R., Maccagni, A. and Grant, J.R. (2017) A Worldwide Molecular Phylogeny Provides New Insight on Cryptic Diversity Within the Moonworts (Botrychium s. S., Ophioglossaceae). *Syst. Bot.*, **42**.

Dauphin, B., Grant, J. and Mráz, P. (2016) Ploidy level and genome size variation in the homosporous ferns Botrychium s.l. (Ophioglossaceae). *Plant Syst. Evol.*, **302**, 575–584.

Dauphin, B., Grant, J.R., Farrar, D.R. and Rothfels, C.J. (2018) Rapid allopolyploid radiation of moonwort ferns (Botrychium; Ophioglossaceae) revealed by PacBio sequencing of homologous and homeologous nuclear regions. *Mol. Phylogenet. Evol.*, **120**, 342–353.

Dauphin, B., Vieu, J. and Grant, J.R. (2014) Molecular phylogenetics supports widespread cryptic species in moonworts (Botrychium s.s., Ophioglossaceae). *Am. J. Bot.*, **101**, 128–140.

DePristo, M.A., Banks, E., Poplin, R., et al. (2011) A framework for variation discovery and genotyping using next-generation DNA sequencing data. *Nat. Genet.*, **43**, 491–498.

Der, J.P., Barker, M.S., Wickett, N.J., dePamphilis, C.W. and Wolf, P.G. (2011) De novo characterization of the gametophyte transcriptome in bracken fern, Pteridium aquilinum. *BMC Genomics*, **12**, 99.

Ellwood, M.D.F. and Foster, W.A. (2004) Doubling the estimate of invertebrate biomass in a rainforest canopy. *Nature*, **429**, 549–551.

Emms, D.M. and Kelly, S. (2015) OrthoFinder: solving fundamental biases in whole genome comparisons dramatically improves orthogroup inference accuracy. *Genome Biol.*, **16**, 157.

Farrar, D.R. (1998) *Population genetics of moonwort Botrychium. In N. Berlin, P. Miller, J. Borovansky, U. S. Seal, and O. Byers [eds.], Population and habitat viability assessment for the goblin fern (Botrychium mormo)*, The Conservation Breeding Specialist Group. Available at: http://www.cpsg.org/content/goblin-fern-phva-1998 [Accessed August 25, 2019].

Field, K.J., Leake, J.R., Tille, S., Allinson, K.E., Rimington, W.R., Bidartondo, M.I., Beerling, D.J. and Cameron, D.D. (2015) From mycoheterotrophy to mutualism: Mycorrhizal specificity and functioning in Ophioglossum vulgatum sporophytes. *New Phytol.*, **205**, 1492–1502.

Gentleman, R. (2020) *annotate: Annotation for microarrays*, Bioconductor version: Release (3.10). Available at: https://bioconductor.org/packages/annotate/ [Accessed February 13, 2020].

George, L.O. and Bazzaz, F.A. (1999a) The Fern Understory as an Ecological Filter: Emergence and Establishment of Canopy-Tree Seedlings. *Ecology*, **80**, 833–845.

George, L.O. and Bazzaz, F.A. (1999b) The Fern Understory as an Ecological Filter: Growth and Survival of Canopy-Tree Seedlings. *Ecology*, **80**, 846–856.

Goudet, J. (2005) hierfstat, a package for r to compute and test hierarchical F-statistics. *Mol. Ecol. Notes*, **5**, 184–186.

Haas, B.J., Papanicolaou, A., Yassour, M., et al. (2013) De novo transcript sequence reconstruction from RNA-seq using the Trinity platform for reference generation and analysis. *Nat. Protoc.*, **8**, 1494–1512.

Haufler, C.H., Pryer, K.M., Schuettpelz, E., Sessa, E.B., Farrar, D.R., Moran, R., Schneller, J.J., Watkins, J.E. and Windham, M.D. (2016) Sex and the Single Gametophyte: Revising the

Homosporous Vascular Plant Life Cycle in Light of Contemporary Research. *BioScience*, **66**, 928–937.

Hauk, W.D. (1995) A Molecular Assessment of Relationships among Cryptic Species of Botrychium Subgenus Botrychium (Ophioglossaceae). *Am. Fern J.*, **85**, 375–394.

Hauk, W.D. and Haufler, C.H. (1999) Isozyme variability among cryptic species of Botrychium subgenus Botrychium (Ophioglossaceae). *Am. J. Bot.*, **86**, 614–633.

Jeffrey, E.C. (1898) The gametophyte of Botrychium virginianum. *Univ Tor. Stud. Biol. Ser.*, **1**, 3-32 pl.i-iv.

Jombart, T. and Ahmed, I. (2011) adegenet 1.3-1: new tools for the analysis of genome-wide SNP data. *Bioinformatics*, **27**, 3070–3071.

Katoh, K., Misawa, K., Kuma, K. and Miyata, T. (2002) MAFFT: a novel method for rapid multiple sequence alignment based on fast Fourier transform. *Nucleic Acids Res.*, **30**, 3059–3066.

Katoh, K. and Standley, D.M. (2013) MAFFT Multiple Sequence Alignment Software Version 7: Improvements in Performance and Usability. *Mol. Biol. Evol.*, **30**, 772–780.

Kearse, M., Moir, R., Wilson, A., et al. (2012) Geneious Basic: an integrated and extendable desktop software platform for the organization and analysis of sequence data. *Bioinforma. Oxf. Engl.*, **28**, 1647–1649.

Kenrick, P. and Crane, P.R. (1997) The origin and early evolution of plants on land. *Nature*, **389**, 33–39.

Khandelwal, S. (1990) Chromosome evolution in the genus Ophioglossum L. *Bot. J. Linn. Soc.*, **102**, 205–217.

Klaus, M., Lawrence R., W., Joanne M., S., Michael, K., Sarah J., R., Peter, H., Roderick, R. and Elizabeth, S. (2010) *Fern ecology*, Cambridge University Press. Available at: https://www.cambridge.org/ch/academic/subjects/life-sciences/plant-science/fern-ecology [Accessed August 8, 2019].

Knaus, B.J. and Grünwald, N.J. (2017) vcfr: a package to manipulate and visualize variant call format data in R. *Mol. Ecol. Resour.*, **17**, 44–53.

Knie, N., Fischer, S., Grewe, F., Polsakiewicz, M. and Knoop, V. (2015) Horsetails are the sister group to all other monilophytes and Marattiales are sister to leptosporangiate ferns. *Mol. Phylogenet. Evol.*, **90**, 140–149.

Kozlov, A.M., Darriba, D., Flouri, T., Morel, B. and Stamatakis, A. (2019) RAxML-NG: a fast, scalable and user-friendly tool for maximum likelihood phylogenetic inference. *Bioinformatics*, **35**, 4453–4455.

Kranz, H.D. and Huss, V.A.R. (1996) Molecular evolution of pteridophytes and their relationship to seed plants: Evidence from complete 18S rRNA gene sequences. *Plant Syst. Evol.*, **202**, 1–11.

Langmead, B. (2010) Aligning Short Sequencing Reads with Bowtie. *Curr. Protoc. Bioinforma.*, **32**, 11.7.1-11.7.14.

Le, S.Q. and Gascuel, O. (2008) An Improved General Amino Acid Replacement Matrix. *Mol. Biol. Evol.*, **25**, 1307–1320.

Leebens-Mack, J.H., Barker, M.S., Carpenter, E.J., et al. (2019) One thousand plant transcriptomes and the phylogenomics of green plants. *Nature*. Available at: https://doi.org/10.1038/s41586-019-1693-2.

Li, F.-W., Brouwer, P., Carretero-Paulet, L., et al. (2018) Fern genomes elucidate land plant evolution and cyanobacterial symbioses. *Nat. Plants*, **4**, 460–472.

Li, H. (2011) A statistical framework for SNP calling, mutation discovery, association mapping and population genetical parameter estimation from sequencing data. *Bioinformatics*, **27**, 2987–2993.

Li, H., Handsaker, B., Wysoker, A., et al. (2009) The Sequence Alignment/Map format and SAMtools. *Bioinforma. Oxf. Engl.*, **25**, 2078–2079.

Maccagni, A., Parisod, C. and Grant, J.R. (2017) Phylogeography of the moonwort fern Botrychium lunaria (Ophioglossaceae) based on chloroplast DNA in the Central-European Mountain System. *Alp. Bot.*, **127**, 185–196.

Marchant, D.B., Sessa, E.B., Wolf, P.G., Heo, K., Barbazuk, W.B., Soltis, P.S. and Soltis, D.E. (2019) The C-Fern (Ceratopteris richardii) genome: insights into plant genome evolution with the first partial homosporous fern genome assembly. *Sci. Rep.*, **9**, 1–14.

Matasci, N., Hung, L.-H., Yan, Z., et al. (2014) Data access for the 1,000 Plants (1KP) project. *GigaScience*, **3**, 17.

McKenna, A., Hanna, M., Banks, E., et al. (2010) The Genome Analysis Toolkit: A MapReduce framework for analyzing next-generation DNA sequencing data. *Genome Res.*, **20**, 1297–1303.

Mirarab, S., Reaz, R., Bayzid, Md.S., Zimmermann, T., Swenson, M.S. and Warnow, T. (2014) ASTRAL: genome-scale coalescent-based species tree estimation. *Bioinformatics*, **30**, i541–i548.

Morgan, M., Falcon, S. and Gentleman, R. (2020) *GSEABase: Gene set enrichment data structures and methods*, Bioconductor version: Release (3.10). Available at: https://bioconductor.org/packages/GSEABase/ [Accessed February 13, 2020].

Obermayer, R., Leitch, I.J., Hanson, L. and Bennett, M.D. (2002) Nuclear DNA C-values in 30 species double the familial representation in pteridophytes. *Ann. Bot.*, **90**, 209–217.

Page, C.N. (2002) Ecological strategies in fern evolution: a neopteridological overview. *Rev. Palaeobot. Palynol.*, **119**, 1–33.

Pagès, H., Carlson, M., Falcon, S. and Li, N. (2020) *AnnotationDbi: Manipulation of SQLite-based annotations in Bioconductor*, Bioconductor version: Release (3.10).

Peterson, B.K., Weber, J.N., Kay, E.H., Fisher, H.S. and Hoekstra, H.E. (2012) Double digest RADseq: an inexpensive method for de novo SNP discovery and genotyping in model and non-model species. *PLoS One*, **7**, e37135.

PPG I (2016) A community-derived classification for extant lycophytes and ferns. *J. Syst. Evol.*, **54**, 563–603.

Pryer, K.M., Schneider, H., Smith, A.R., Cranfill, R., Wolf, P.G., Hunt, J.S. and Sipes, S.D. (2001) Horsetails and ferns are a monophyletic group and the closest living relatives to seed plants. *Nature*, **409**, 618–622.

Pryer, K.M., Schuettpelz, E., Wolf, P.G., Schneider, H., Smith, A.R. and Cranfill, R. (2004) Phylogeny and evolution of ferns (monilophytes) with a focus on the early leptosporangiate divergences. *Am. J. Bot.*, **91**, 1582–1598.

R Development Core Team (2020) R: The R Project for Statistical Computing. Available at: https://www.r-project.org/ [Accessed February 9, 2020].

Rai, H.S. and Graham, S.W. (2010) Utility of a large, multigene plastid data set in inferring higher-order relationships in ferns and relatives (monilophytes). *Am. J. Bot.*, **97**, 1444–1456.

Rambaud, A. (2009) FigTree 1.4.4. Available at: http://tree.bio.ed.ac.uk/software/figtree/ [Accessed January 17, 2020].

Ranker, T.A. and Haufler, C.H. (2008) *Biology and Evolution of Ferns and Lycophytes*, Cambridge University Press. Available at: /core/books/biology-and-evolution-of-ferns-and-lycophytes/B8C92258A68F155B3A7DBBFB84D0B48F [Accessed August 8, 2019].

Raubeson, L.A. and Jansen, R.K. (1992) Chloroplast DNA evidence on the ancient evolutionary split in vascular land plants. *Science*, **255**, 1697–1699.

Rellstab, C., Zoller, S., Walthert, L., et al. (2016) Signatures of local adaptation in candidate genes of oaks (Quercus spp.) with respect to present and future climatic conditions. *Mol. Ecol.*, **25**, 5907–5924.

Rogivue, A., Choudhury, R.R., Zoller, S., Joost, S., Felber, F., Kasser, M., Parisod, C. and Gugerli, F. (2019) Genome-wide variation in nucleotides and retrotransposons in alpine populations of Arabis alpina (Brassicaceae). *Mol. Ecol. Resour.*, **19**, 773–787.

Rothfels, C.J., Larsson, A., Li, F.-W., et al. (2013) Transcriptome-Mining for Single-Copy Nuclear Markers in Ferns. *PLOS ONE*, **8**, e76957.

Rothfels, C.J., Li, F.-W., Sigel, E.M., et al. (2015) The evolutionary history of ferns inferred from 25 low-copy nuclear genes. *Am. J. Bot.*, **102**, 1089–1107.

RStudio Team (2015) RStudio: Integrated Development for R. RStudio, Inc., Boston. Available at: https://www.rstudio.com/ [Accessed August 30, 2019].

Sayyari, E. and Mirarab, S. (2016) Fast Coalescent-Based Computation of Local Branch Support from Quartet Frequencies. *Mol. Biol. Evol.*, **33**, 1654–1668.

Schuettpelz, E. and Pryer, K.M. (2007) Fern phylogeny inferred from 400 leptosporangiate species and three plastid genes. *Taxon*, **56**.

Seeb, J.E., Carvalho, G., Hauser, L., Naish, K., Roberts, S. and Seeb, L.W. (2011) Single-nucleotide polymorphism (SNP) discovery and applications of SNP genotyping in nonmodel organisms. *Mol. Ecol. Resour.*, **11**, 1–8.

Seo, T.-K. (2008) Calculating Bootstrap Probabilities of Phylogeny Using Multilocus Sequence Data. *Mol. Biol. Evol.*, **25**, 960–971.

Sessa, E.B., Zimmer, E.A. and Givnish, T.J. (2012) Unraveling reticulate evolution in North American Dryopteris (Dryopteridaceae). *BMC Evol. Biol.*, **12**, 104.

Shen, H., Jin, D., Shu, J.-P., et al. (2017) Large-scale phylogenomic analysis resolves a backbone phylogeny in ferns. *GigaScience*, **7**. Available at: https://www.ncbi.nlm.nih.gov/pmc/articles/PMC5795342/ [Accessed July 22, 2019].

Sigel, E.M., Schuettpelz, E., Pryer, K.M. and Der, J.P. (2018) Overlapping Patterns of Gene Expression Between Gametophyte and Sporophyte Phases in the Fern Polypodium amorphum (Polypodiales). *Front. Plant Sci.*, **9**. Available at: https://www.frontiersin.org/articles/10.3389/fpls.2018.01450/full [Accessed November 3, 2019].

Simão, F.A., Waterhouse, R.M., Ioannidis, P., Kriventseva, E.V. and Zdobnov, E.M. (2015) BUSCO: assessing genome assembly and annotation completeness with single-copy orthologs. *Bioinformatics*, **31**, 3210–3212.

Sloan, D.B., Keller, S.R., Berardi, A.E., Sanderson, B.J., Karpovich, J.F. and Taylor, D.R. (2012) De novo transcriptome assembly and polymorphism detection in the flowering plant Silene vulgaris (Caryophyllaceae). *Mol. Ecol. Resour.*, **12**, 333–343.

Swartz, L.M. and Brunsfeld, S.J. (2002) The morphological and genetic distinctness of Botrychium minganense and B. crenulatum as assessed by morphometric analysis and RAPD markers. *Am. Fern J.*, **92**, 249–269.

Testo, W. and Sundue, M. (2016) A 4000-species dataset provides new insight into the evolution of ferns. *Mol. Phylogenet. Evol.*, **105**, 200–211.

Van der Auwera, G.A., Carneiro, M.O., Hartl, C., et al. (2013) From FastQ data to high confidence variant calls: the Genome Analysis Toolkit best practices pipeline. *Curr. Protoc. Bioinforma.*, **43**, 11.10.1-33.

Walker, L.R. (1994) Effects of fern thickets on woodland development on landslides in Puerto Rico. *J. Veg. Sci.*, **5**, 525–532.

Wickett, N.J., Mirarab, S., Nguyen, N., et al. (2014) Phylotranscriptomic analysis of the origin and early diversification of land plants. *Proc. Natl. Acad. Sci.*, **111**, E4859–E4868.

Wickham, H. (2016) *ggplot2: Elegant Graphics for Data Analysis* 2nd ed., Springer International Publishing. Available at: https://www.springer.com/gp/book/9783319242750 [Accessed January 17, 2020].

Williams, E.W., Farrar, D.R. and Henson, Don (2016) Cryptic speciation in allotetraploids: Lessons from the Botrychium matricariifolium (Ophioglossaceae) complex. *Am. J. Bot.*, **103**, 1–14.

Winther, J.L. and Friedman, W.E. (2007) Arbuscular mycorrhizal symbionts in Botrychium (Ophioglossaceae). *Am. J. Bot.*, **94**, 1248–1255.

Wood, T.E., Takebayashi, N., Barker, M.S., Mayrose, I., Greenspoon, P.B. and Rieseberg, L.H. (2009) The frequency of polyploid speciation in vascular plants. *Proc. Natl. Acad. Sci.*, **106**, 13875–13879.

Yeaman, S., Hodgins, K.A., Lotterhos, K.E., et al. (2016) Convergent local adaptation to climate in distantly related conifers. *Science*, **353**, 1431–1433.

Zhang, C., Rabiee, M., Sayyari, E. and Mirarab, S. (2018) ASTRAL-III: polynomial time species tree reconstruction from partially resolved gene trees. *BMC Bioinformatics*, **19**, 153.

Figures

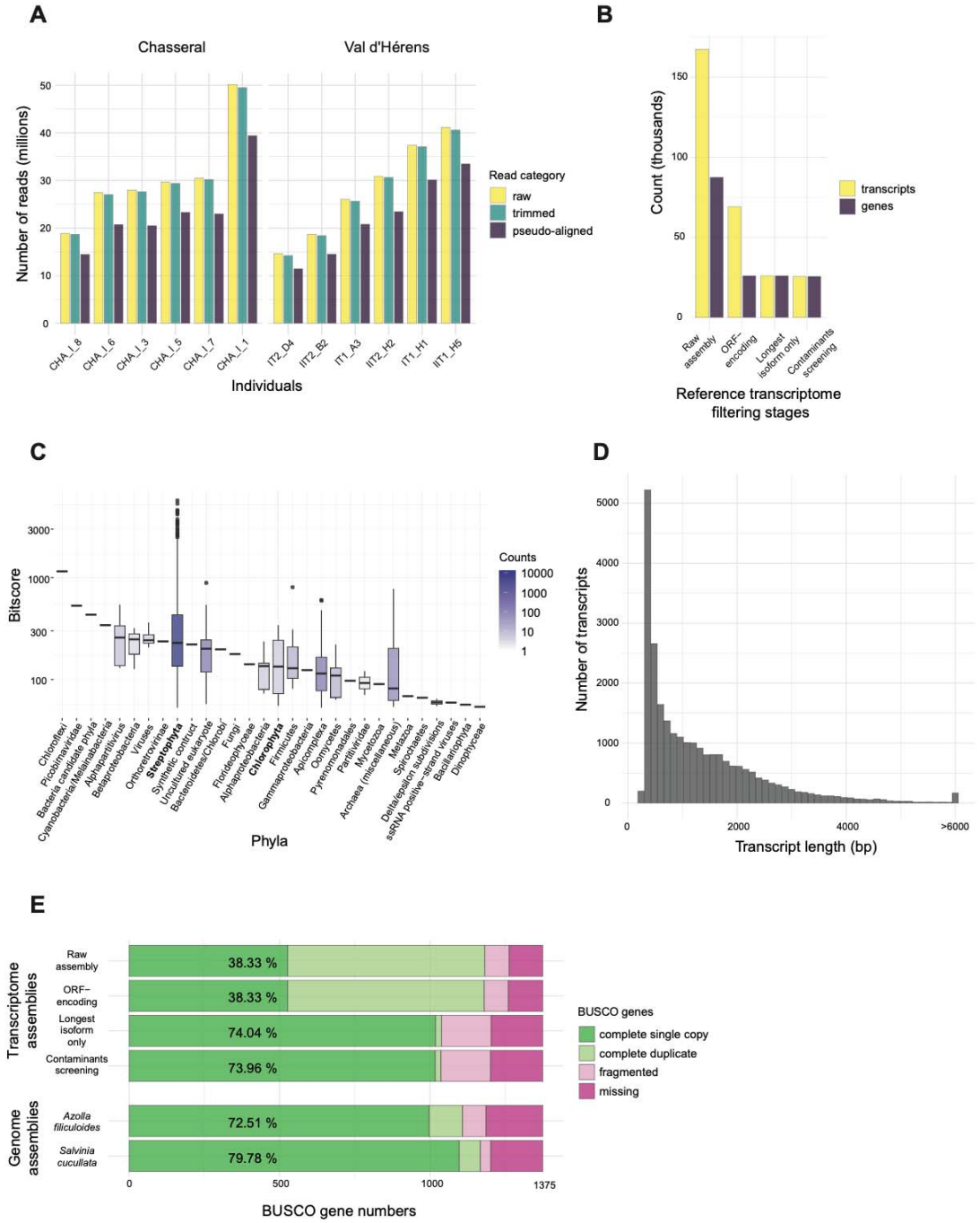

Figure 1: De novo assembly of the *Botrychium lunaria* transcriptome. (A) Distribution of the raw, trimmed, and pseudo-aligned read numbers per individual. (B) Transcripts and gene assembly content at each filtering stage of the reference transcriptome. (C) Contaminant transcript sequences detected by phylum. Retained phyla are indicated in bold. (D) Distribution of the transcript lengths for the reference transcriptome. (E) BUSCO genes detected at each filtering stage of the *B. lunaria* transcriptome and for two genome assemblies of ferns (*Azolla filliculoides* and *Salvinia cucullata*) (Li *et al.*, 2018).

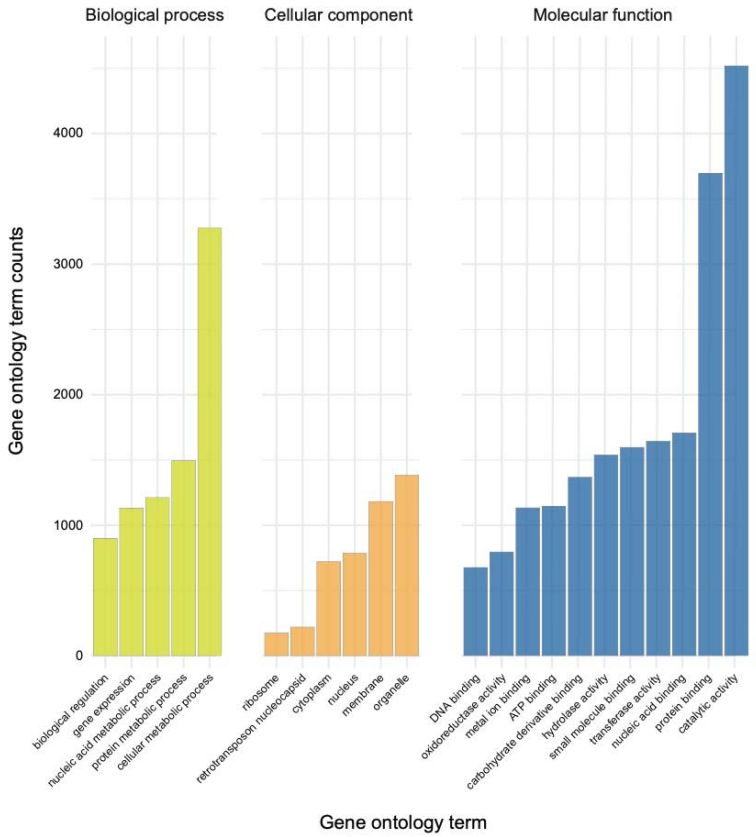

Figure 2: Characterizations of predicted functions encoded by the transcriptome. Gene ontology (GO) term annotations are shown for the 30 most frequent terms per ontology (BP, CC, and MF). GO terms with highly similar functions are excluded from the representation.

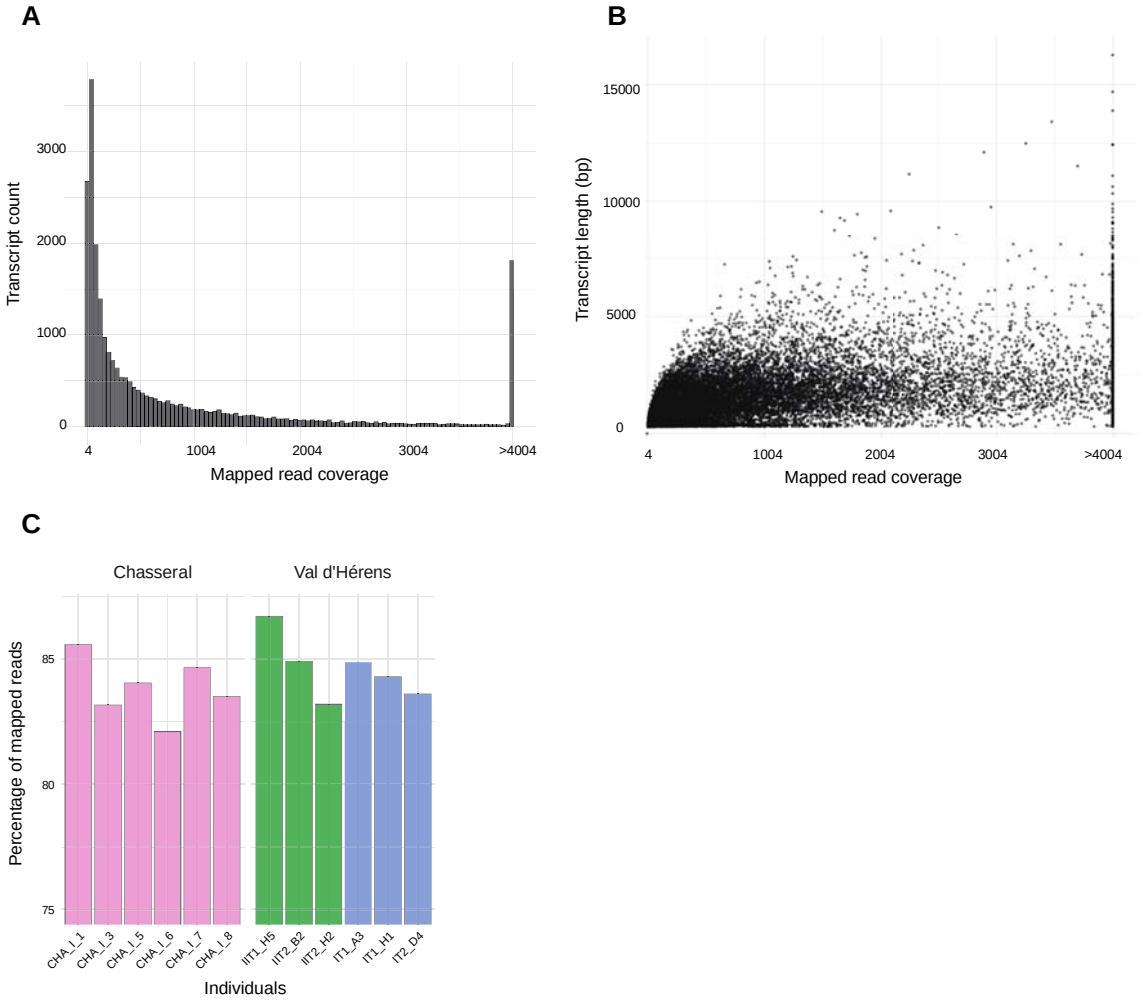

Figure 3: Analyses of the assembly coverage. (A) Number of aligned reads per assembled transcript for the reference individual. (B) Aligned reads of the reference individual according to the assembled transcript length. (C) Mapping rate of all 12 individuals from the Chasseral and Val d'Hérens populations (including the subpopulations Forclaz and Mase). The reference individual used to assemble the transcriptome was CHA_I_1.

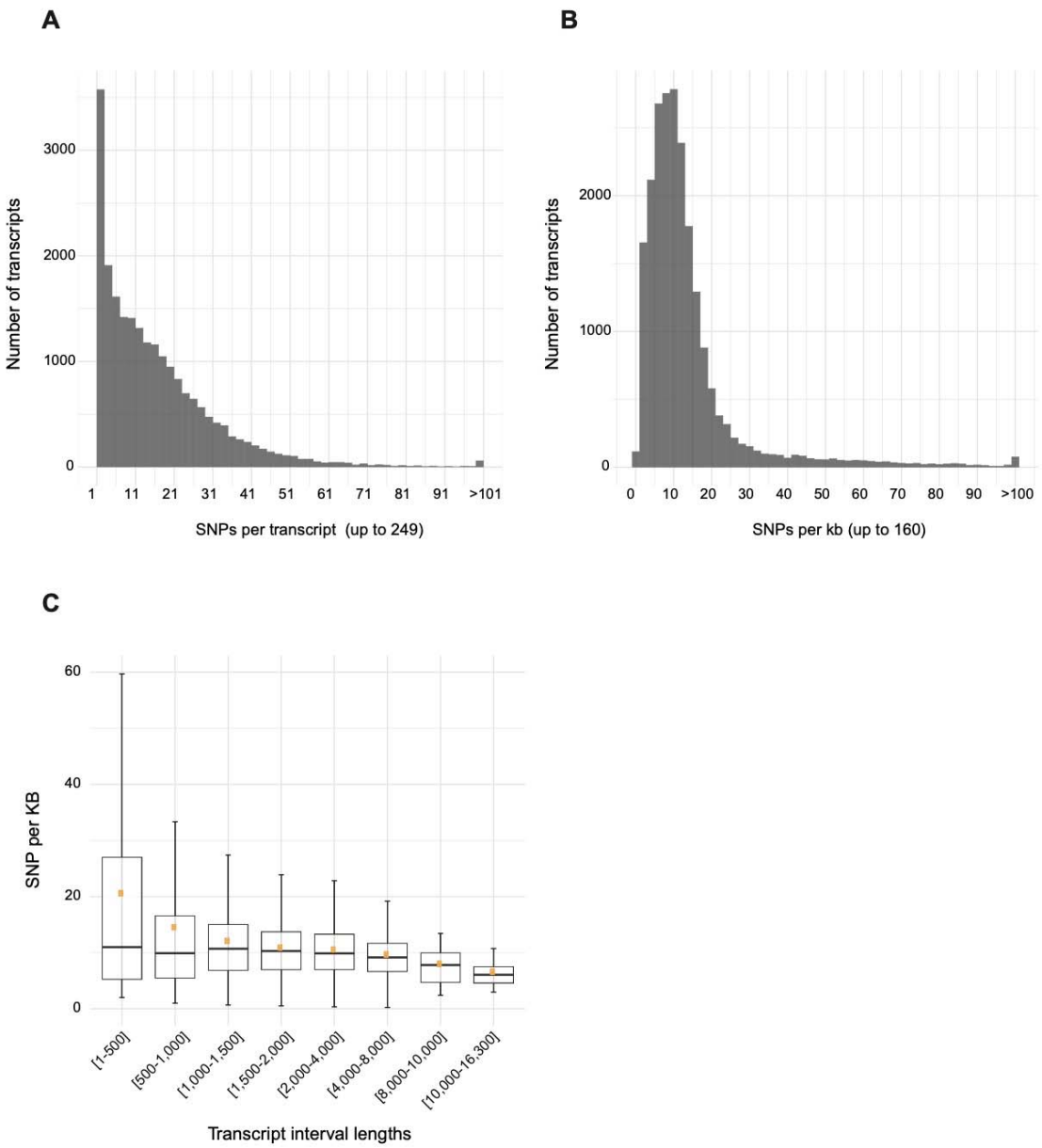

Figure 4: Analyses of population-level transcriptomic polymorphism. (A) Number of SNPs per transcript. (B) Density of SNPs per transcript (number of SNPs per kb). (C) SNP density according to bins of transcript length. The mean density is shown by an orange rectangle.

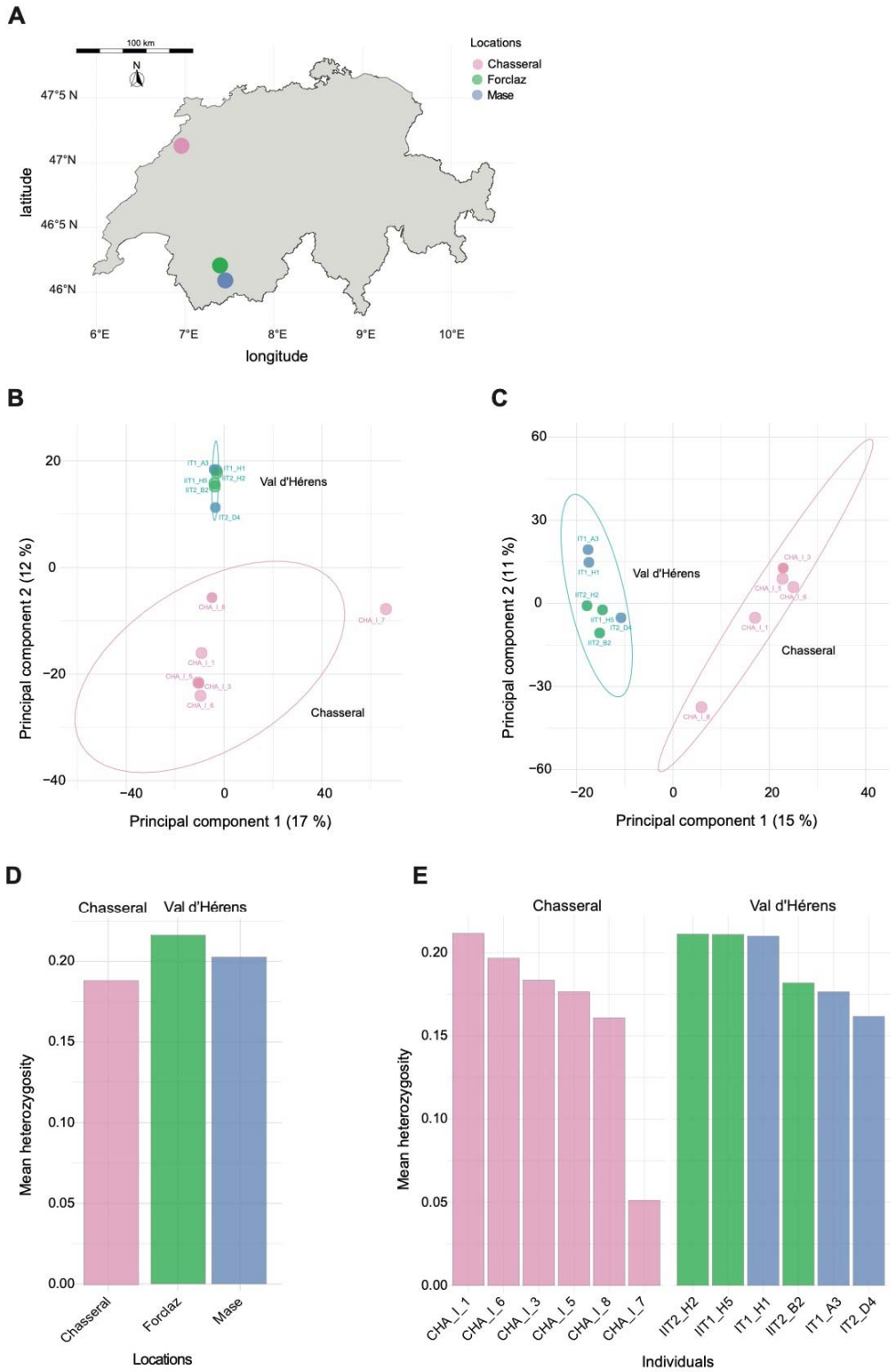

Figure 5: Population genetic structure and observed heterozygosity. (A) Principal component analysis (PCA) of the populations Chasseral and Val d'Hérens (sites Mase and Forclaz). (B) PCA of both populations excluding the CHA_I_7 outlier. Both PCA were analyzed using a reduced SNP dataset of a maximum of 1 SNP per kb of transcript. (C) Mean observed heterozygosity per location grouped by population. (D) Mean observed heterozygosity per individual grouped by population.

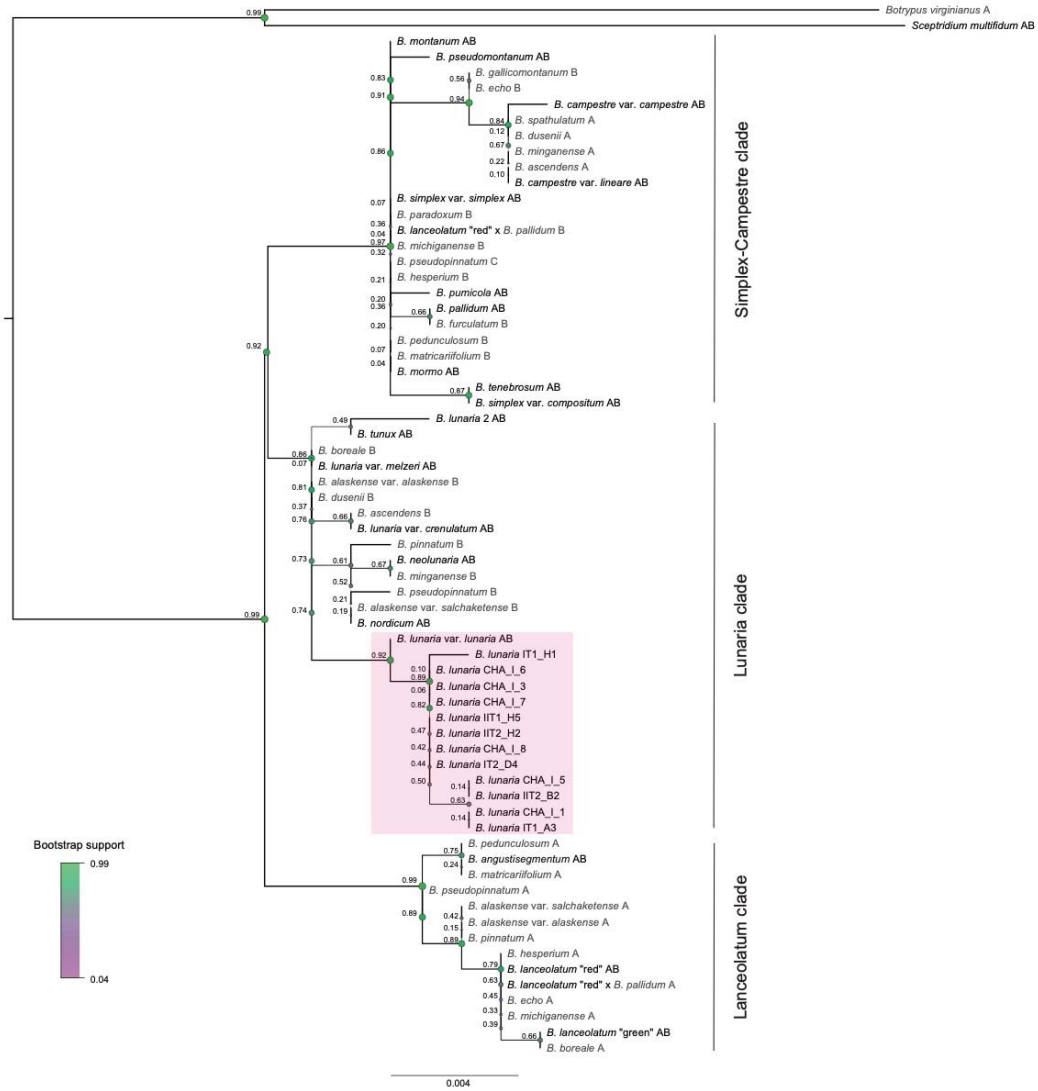

Figure 6: Phylogenetic positions of the *Botrychium lunaria* samples from Chasseral and Val d'Hérens within *Botrychium* genus. Rooted maximum likelihood (ML) tree of the CRY2cA locus. ML bootstrap support values are shown above branches. Thicker branch lines, larger node sizes and nodes colored in green further indicate higher bootstrap values. Diploid taxa are shown in black and polyploids are shown in grey. For polyploids, the subgenome is shown individually on the tree and specified by a letter after the species name: "A" for maternal subgenome, "B" for paternal subgenome, and "C" for additional subgenome for the hexaploid (modified from Dauphin *et al.*, 2018). The three *Botrychium* main clades were delimited by black lines. Individuals from Chasseral and Val d'Hérens populations are highlighted by a pink rectangle.

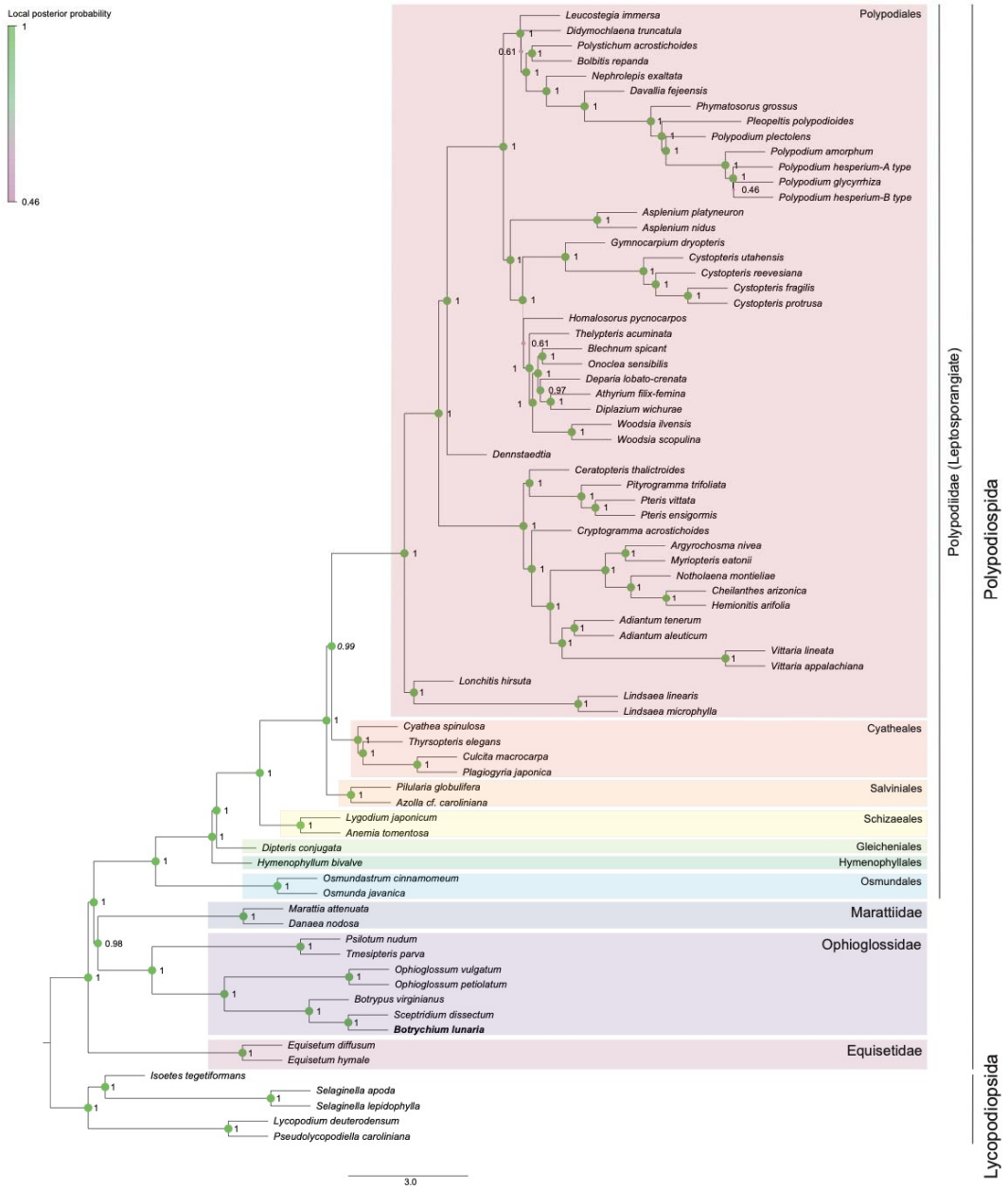

Figure 7 Phylogenomic relationships among ferns including *Botrychium lunaria* . A consensus tree of 864 orthologous genes including 74 taxa was built using ASTRAL. The branch support is indicated by local posterior probability values on node sides. Thicker branch lines, larger node sizes and nodes colored in green further indicate higher local posterior probability values. The delimitation between outgroups (Lycopodiopsida) and ferns (Polypodiopsida) is shown by black lines. Fern subclasses (Equisetidae, Ophioglossidae, Marattiidae and Polypodiidae) are denoted by colored rectangles or a black line on the clade side. Polypodiidae orders (Osmundales, Hymenophyllales, Gleicheniales, Schizaeales Salviniales, Cyatheales and Polypodiales) are designated by colored rectangles.

Tables

Table 1: Overview of assembly statistics over the different transcript filtering stages.

Filtering stage	Assembled bases	Transcripts	Genes	N50-longest isoform	N50-all	GC%
Raw assembly	56,273,802	167,306	87,537	1,689	1,089	43.68
ORF-encoding	34,588,465	69,280	26,139	2,152	1,988	44.00
Longest isoform only	34,588,465	26,139	26,139	1,988	1,988	44.31
Contaminants screening	34,255,139	25,721	25,721	1,995	1,995	44.30

Table 2: Analyses of assembly completeness using BUSCO genes. The *B. lunaria* transcriptome is compare to two genome assemblies of ferns (*Azolla filliculoides* and *Salvinia cucullata*).

Species name	Filtering stage	C[1]	CS[2]	CD[3]	F[4]	M[5]	n[6]	dataset
Azolla filliculoides	-	1,108	997	111	78	189	1,375	embryophyta_odb10
Salvinia cucullata	-	1,167	1097	70	35	173	1,375	embryophyta_odb10
B. lunaria	Raw assembly	1,182	527	655	81	112	1,375	embryophyta_odb10
B. lunaria	ORF-encoding	1,180	527	653	80	115	1,375	embryophyta_odb10
B. lunaria	Longest isoform only	1,038	1,018	20	165	172	1,375	embryophyta_odb10
B. lunaria	Contaminants screening	1,036	1,017	19	165	174	1,375	embryophyta_odb10

Note: [1]Complete genes, [2]Complete and single copy genes, [3]Complete and duplicated genes, [4]Fragmented genes, [5]Missing genes, [6]Total number of BUSCO genes in the dataset.

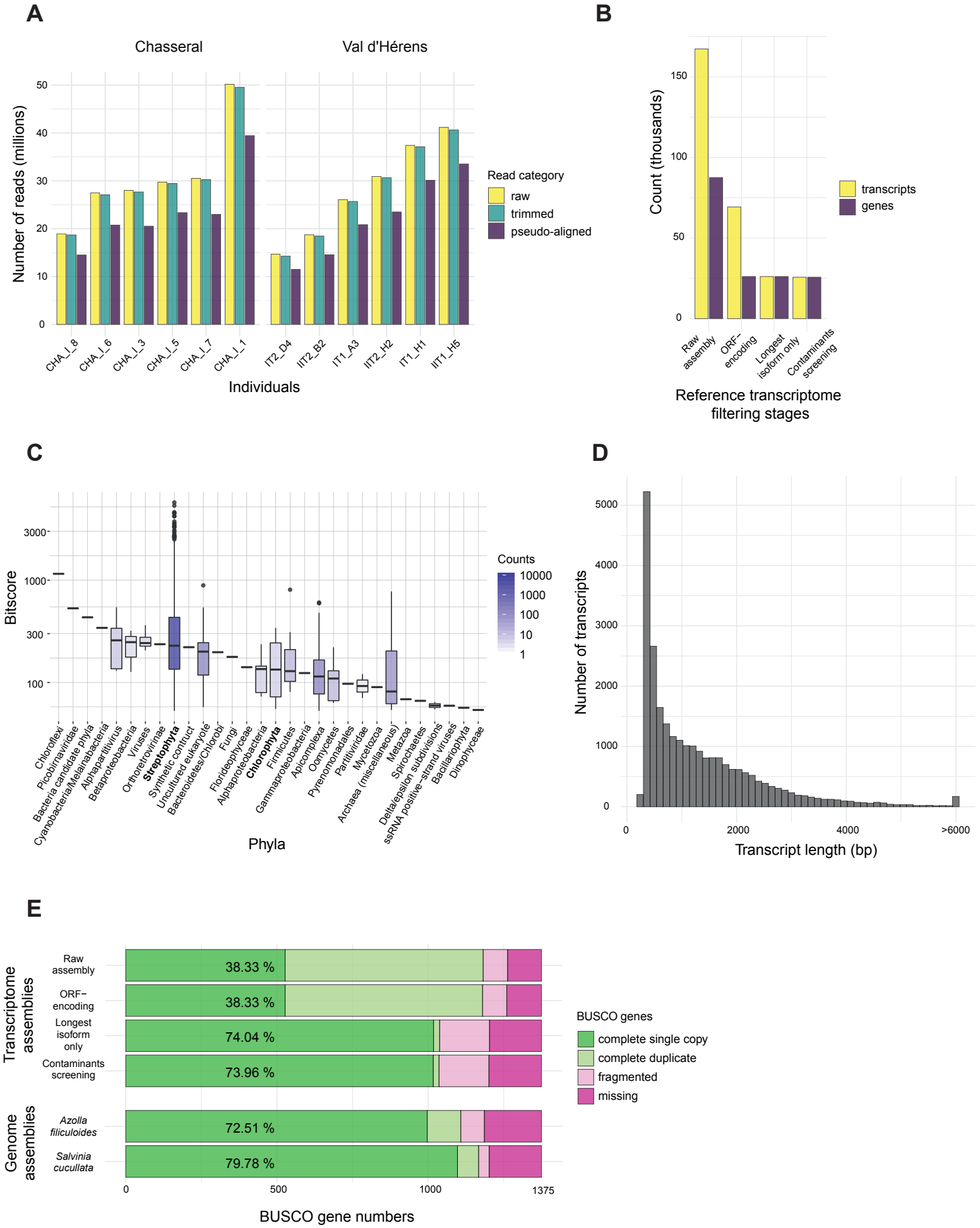
A
Chasseral
Val d'Hérens
Number of reads (millions)
0
10
20
30
40
50
CHA_I_8
CHA_I_6
CHA_I_3
CHA_I_5
CHA_I_7
CHA_I_1
IT2_D4
IIT2_B2
IT1_A3
IIT2_H2
IT1_H1
IIT1_H5
Individuals
Read category
raw
trimmed
pseudo-aligned
B
Count (thousands)
0
50
100
150
Raw assembly
ORF-encoding
Longest isoform only
Contaminants screening
Reference transcriptome filtering stages
transcripts
genes
C
Bitscore
100
300
1000
3000
Chloroflexi
Picobirnaviridae
Bacteria candidate phyla
Cyanobacteria/Melainabacteria
Alphapartitivirus
Betaproteobacteria
Viruses
Orthoretrovirinae
Streptophyta
Synthetic contruct
Uncultured eukaryote
Bacteroidetes/Chlorobi
Fungi
Florideophyceae
Alphaproteobacteria
Chlorophyta
Firmicutes
Gammaproteobacteria
Apicomplexa
Oomycetes
Pyrenomonadales
Partitiviridae
Mycetozoa
Archaea (miscellaneous)
Metazoa
Spirochaetes
Deltaepsilon subdivisions
ssRNA positive-strand viruses
Bacillariophyta
Dinophyceae
Phyla
Counts
10000
1000
100
10
1
D
Number of transcripts
0
1000
2000
3000
4000
5000
0
2000
4000
>6000
Transcript length (bp)
E
Transcriptome assemblies
Raw assembly
ORF-encoding
Longest isoform only
Contaminants screening
38.33 %
38.33 %
74.04 %
73.96 %
Genome assemblies
Azolla filiculoides
Salvinia cucullata
72.51 %
79.78 %
0
500
1000
1375
BUSCO gene numbers
BUSCO genes
complete single copy
complete duplicate
fragmented
missing

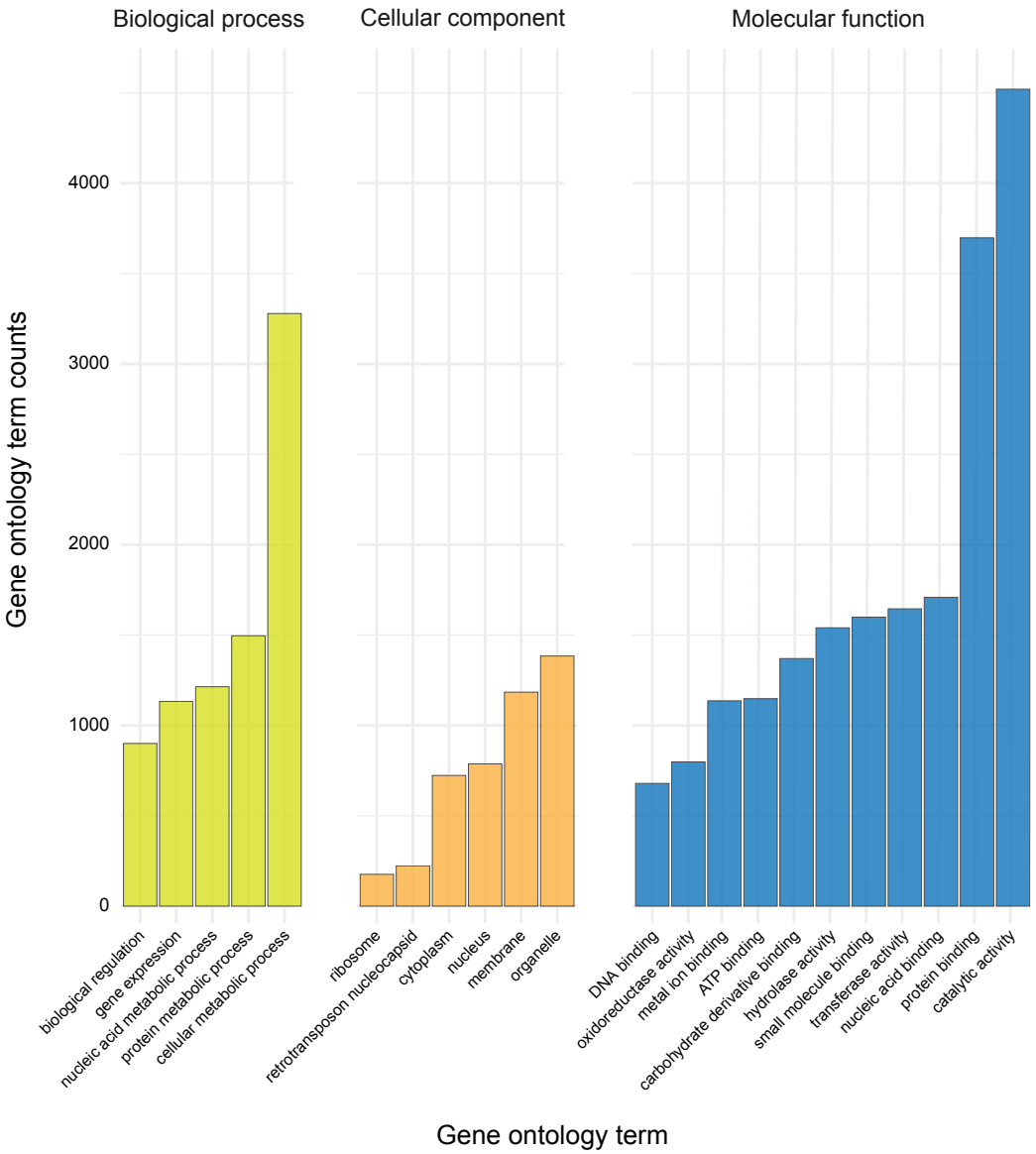
Biological process
Cellular component
Molecular function
Gene ontology term counts
4000
3000
2000
1000
0
biological regulation
gene expression
nucleic acid metabolic process
protein metabolic process
cellular metabolic process
ribosome
retrotransposon nucleocapsid
cytoplasm
nucleus
membrane
organelle
DNA binding
oxidoreductase activity
metal ion binding
ATP binding
carbohydrate derivative binding
hydrolase activity
small molecule binding
transferase activity
nucleic acid binding
protein binding
catalytic activity
Gene ontology term

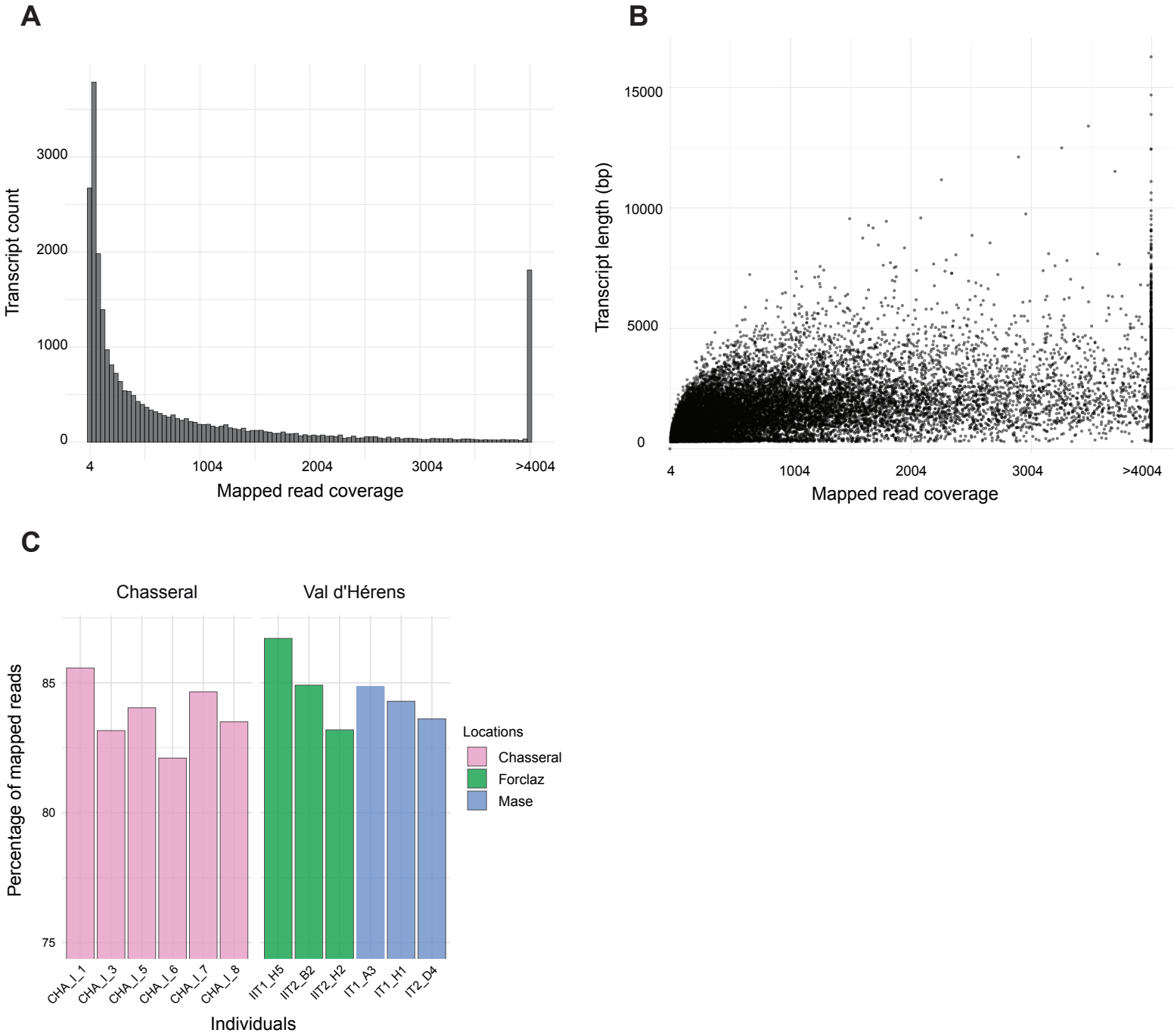
A
Transcript count
3000
2000
1000
0
4
1004
2004
3004
>4004
Mapped read coverage
B
Transcript length (bp)
15000
10000
5000
0
4
1004
2004
3004
>4004
Mapped read coverage
C
Chasseral
Val d'Hérens
Percentage of mapped reads
85
80
75
CHA_I_1
CHA_I_3
CHA_I_5
CHA_I_6
CHA_I_7
CHA_I_8
IIT1_H5
IIT2_B2
IIT2_H2
IT1_A3
IT1_H1
IT2_D4
Individuals
Locations
Chasseral
Forclaz
Mase

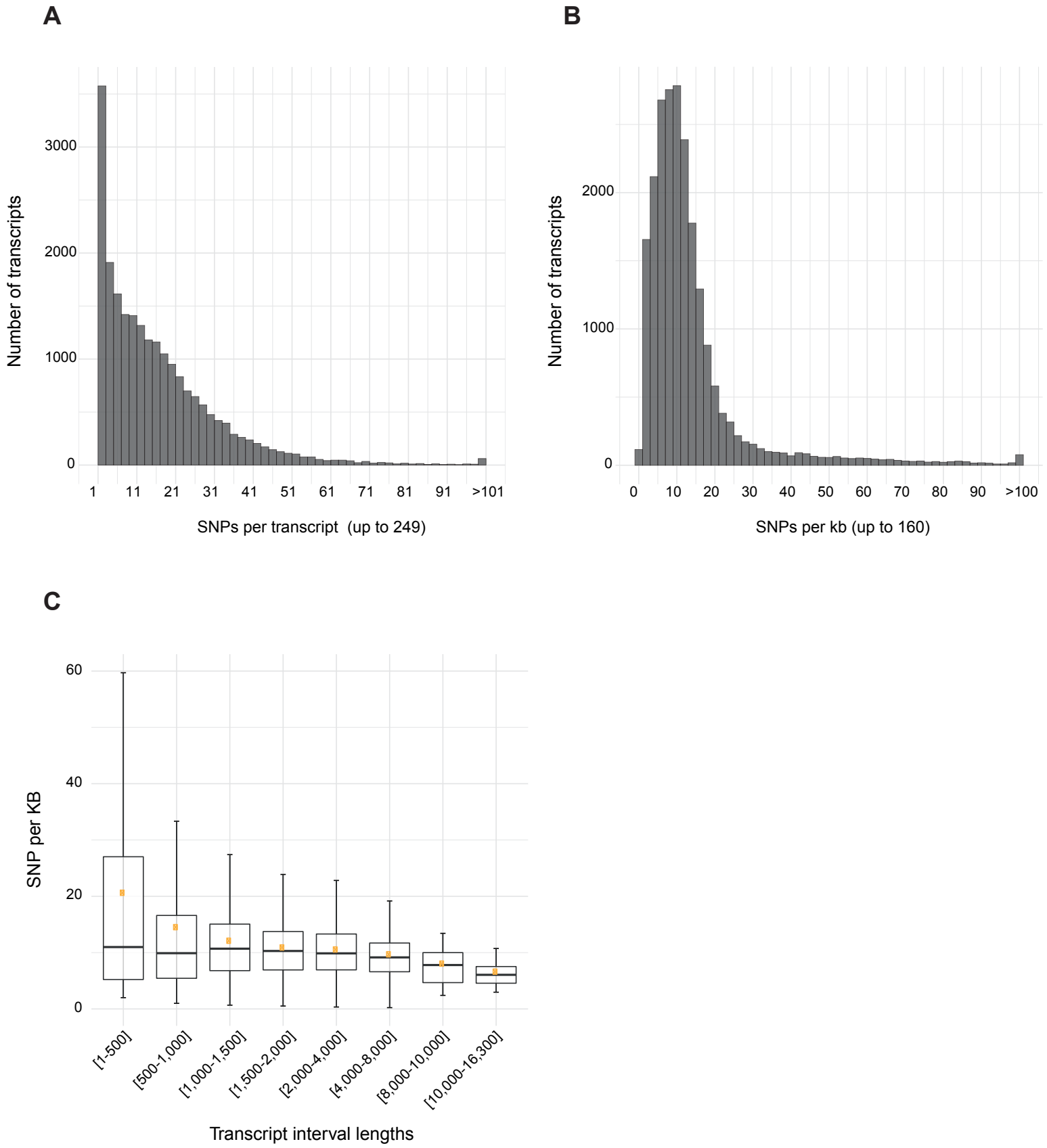
A
Number of transcripts
3000
2000
1000
0
1
11
21
31
41
51
61
71
81
91
>101
SNPs per transcript (up to 249)
B
Number of transcripts
2000
1000
0
0
10
20
30
40
50
60
70
80
90
>100
SNPs per kb (up to 160)
C
SNP per KB
60
40
20
0
[1-500]
[500-1,000]
[1,000-1,500]
[1,500-2,000]
[2,000-4,000]
[4,000-8,000]
[8,000-10,000]
[10,000-16,300]
Transcript interval lengths

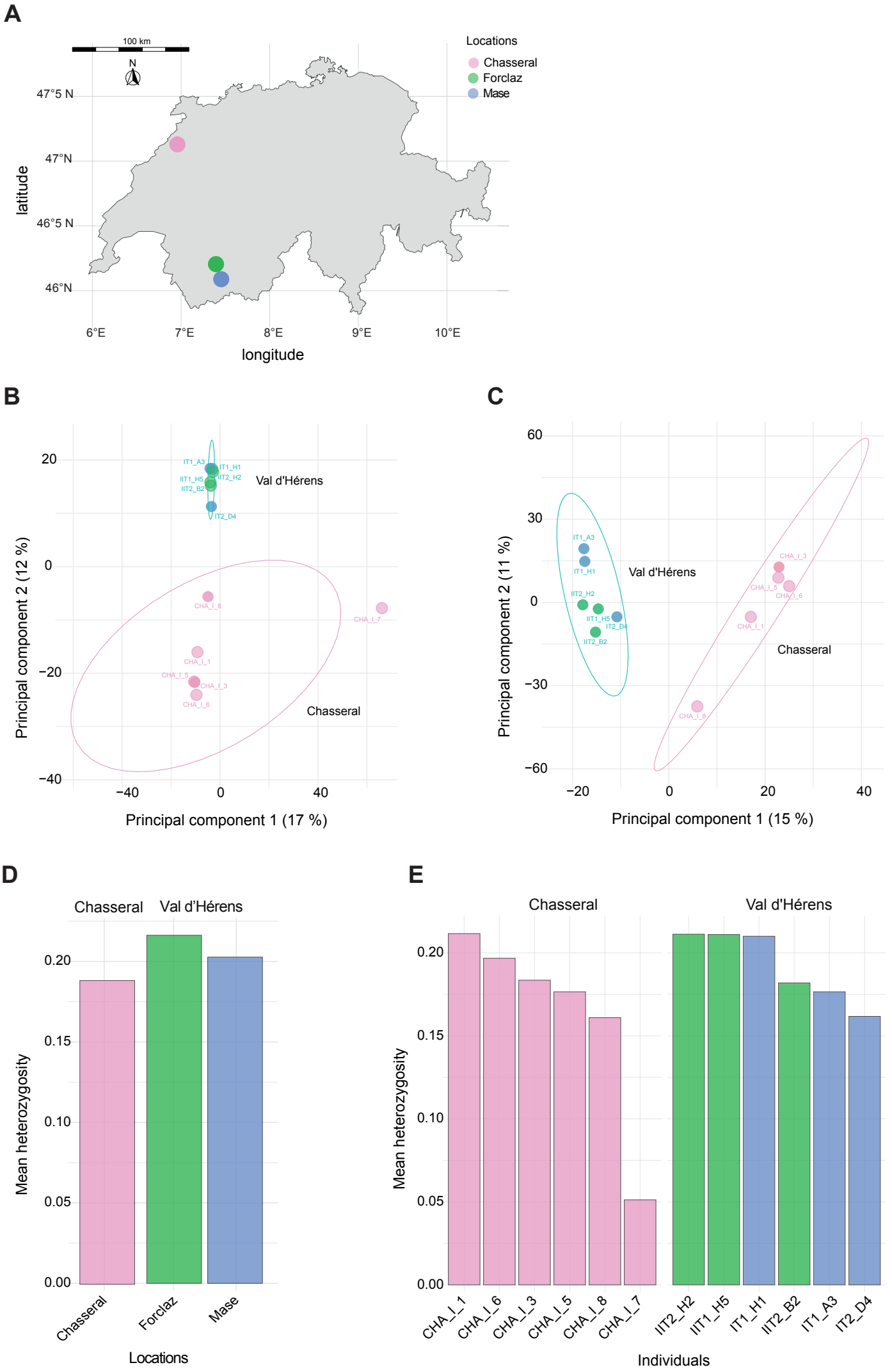
A
100 km
N
Locations
Chasseral
Forclaz
Mase
47°5 N
47°N
46°5 N
46°N
latitude
6°E
7°E
8°E
9°E
10°E
longitude
B
Val d'Hérens
Chasseral
Principal component 2 (12 %)
Principal component 1 (17 %)
C
Val d'Hérens
Chasseral
Principal component 2 (11 %)
Principal component 1 (15 %)
D
Chasseral
Val d'Hérens
Mean heterozygosity
Chasseral
Forclaz
Mase
Locations
E
Chasseral
Val d'Hérens
Mean heterozygosity
CHA_I_1
CHA_I_6
CHA_I_3
CHA_I_5
CHA_I_8
CHA_I_7
IIT2_H2
IIT1_H5
IT1_H1
IIT2_B2
IT1_A3
IT2_D4
Individuals

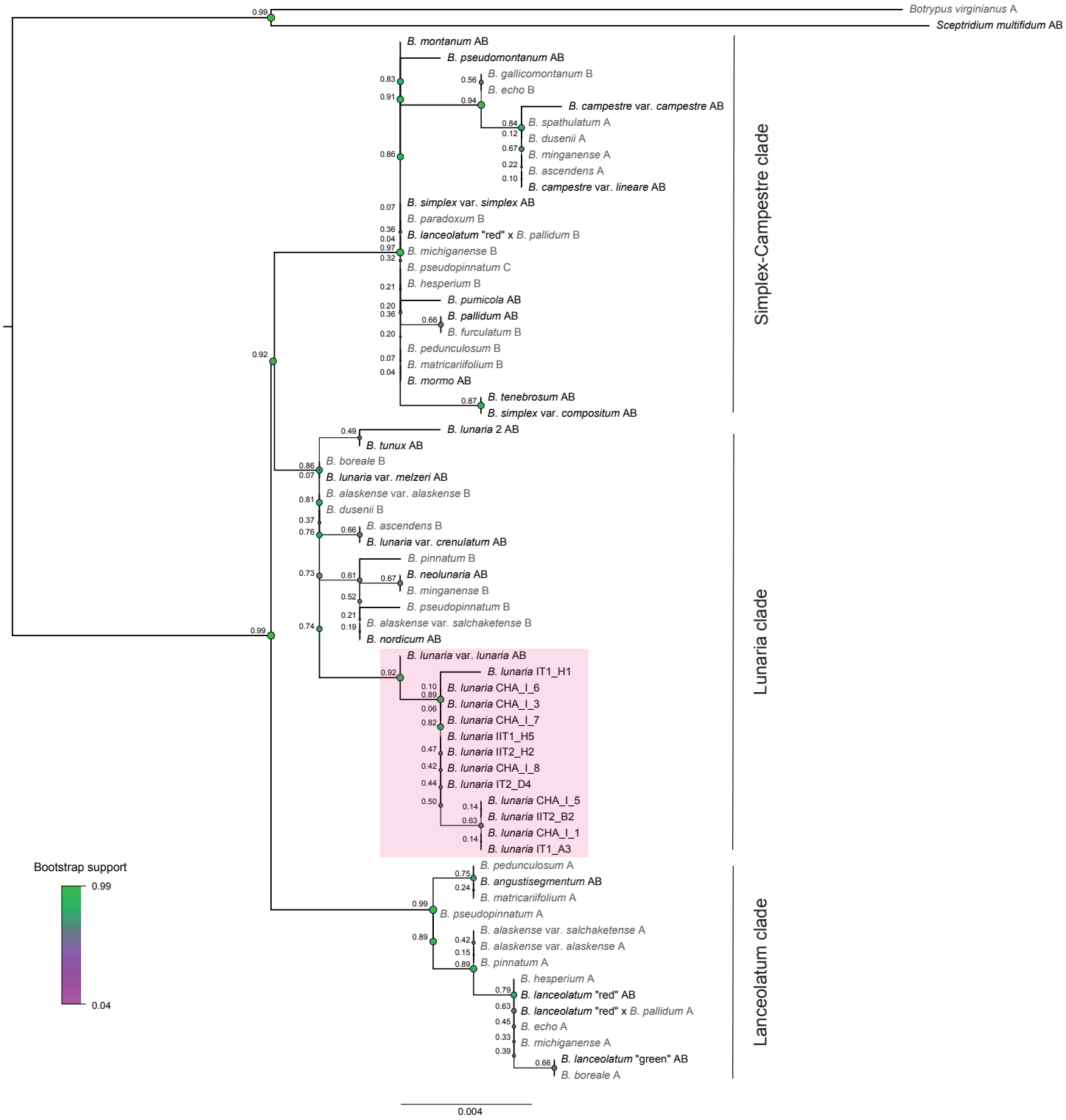
Botrypus virginianus A
Sceptridium multifidum AB
B. montanum AB
B. pseudomontanum AB
B. gallicomontanum B
B. echo B
B. campestre var. campestre AB
B. spathulatum A
B. dusenii A
B. minganense A
B. ascendens A
B. campestre var. lineare AB
B. simplex var. simplex AB
B. paradoxum B
B. lanceolatum "red" x B. pallidum B
B. michiganense B
B. pseudopinnatum C
B. hesperium B
B. pumicola AB
B. pallidum AB
B. furculatum B
B. pedunculosum B
B. matricariifolium B
B. mormo AB
B. tenebrosum AB
B. simplex var. compositum AB
Simplex-Campestre clade
B. lunaria 2 AB
B. tunux AB
B. boreale B
B. lunaria var. melzeri AB
B. alaskense var. alaskense B
B. dusenii B
B. ascendens B
B. lunaria var. crenulatum AB
B. pinnatum B
B. neolunaria AB
B. minganense B
B. pseudopinnatum B
B. alaskense var. salchaketense B
B. nordicum AB
B. lunaria var. lunaria AB
B. lunaria IT1_H1
B. lunaria CHA_I_6
B. lunaria CHA_I_3
B. lunaria CHA_I_7
B. lunaria IIT1_H5
B. lunaria IIT2_H2
B. lunaria CHA_I_8
B. lunaria IT2_D4
B. lunaria CHA_I_5
B. lunaria IIT2_B2
B. lunaria CHA_I_1
B. lunaria IT1_A3
Lunaria clade
B. pedunculosum A
B. angustisegmentum AB
B. matricariifolium A
B. pseudopinnatum A
B. alaskense var. salchaketense A
B. alaskense var. alaskense A
B. pinnatum A
B. hesperium A
B. lanceolatum "red" AB
B. lanceolatum "red" x B. pallidum A
B. echo A
B. michiganense A
B. lanceolatum "green" AB
B. boreale A
Lanceolatum clade
Bootstrap support
0.99
0.04
0.004

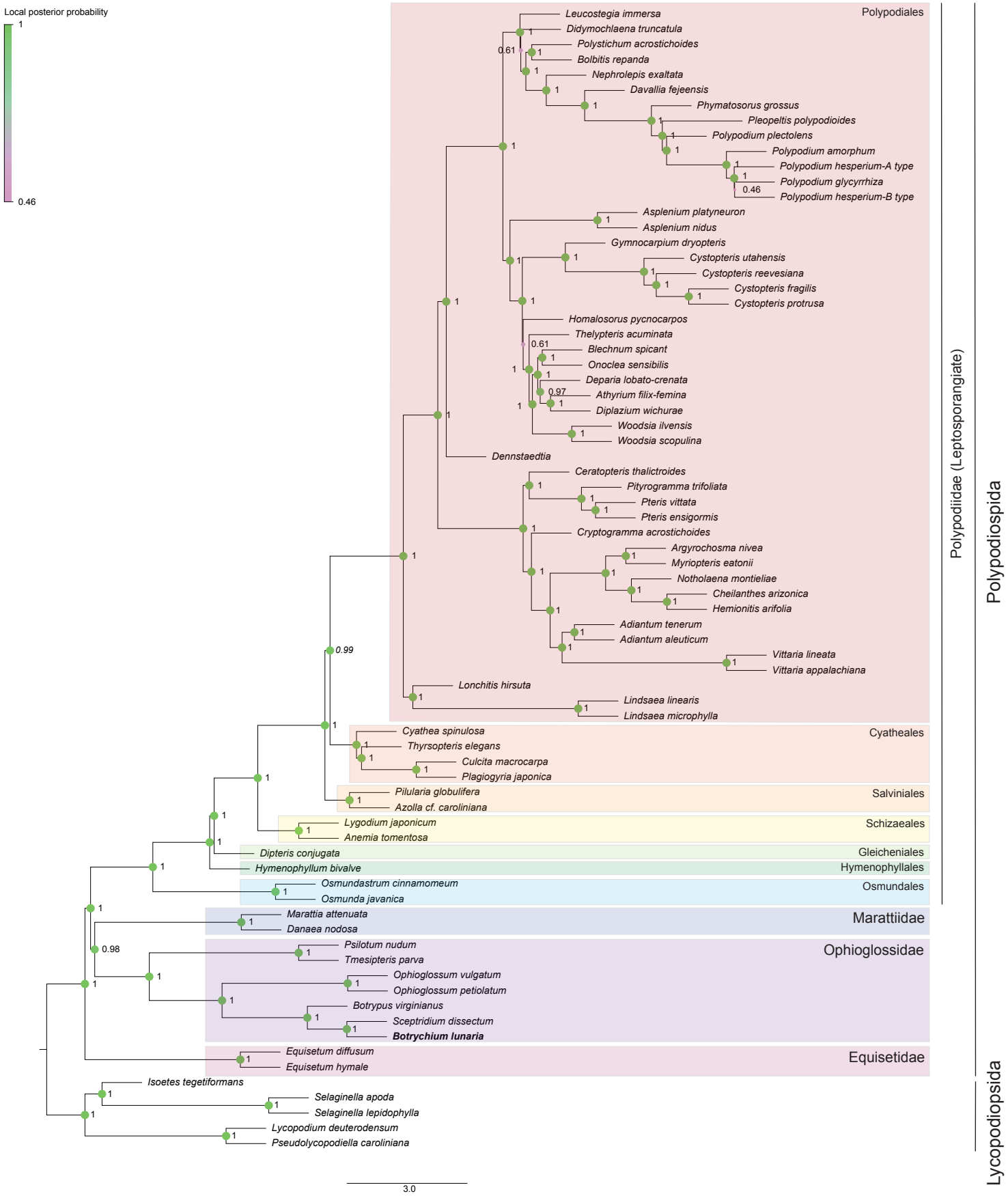
Local posterior probability
1
0.46
Polypodiales
Leucostegia immersa
Didymochlaena truncatula
Polystichum acrostichoides
Bolbitis repanda
Nephrolepis exaltata
Davallia fejeensis
Phymatosorus grossus
Pleopeltis polypodioides
Polypodium plectolens
Polypodium amorphum
Polypodium hesperium-A type
Polypodium glycyrrhiza
Polypodium hesperium-B type
Asplenium platyneuron
Asplenium nidus
Gymnocarpium dryopteris
Cystopteris utahensis
Cystopteris reevesiana
Cystopteris fragilis
Cystopteris protrusa
Homalosorus pycnocarpos
Thelypteris acuminata
Blechnum spicant
Onoclea sensibilis
Deparia lobato-crenata
Athyrium filix-femina
Diplazium wichurae
Woodsia ilvensis
Woodsia scopulina
Dennstaedtia
Ceratopteris thalictroides
Pityrogramma trifoliata
Pteris vittata
Pteris ensigormis
Cryptogramma acrostichoides
Argyrochosma nivea
Myriopteris eatonii
Notholaena montieliae
Cheilanthes arizonica
Hemionitis arifolia
Adiantum tenerum
Adiantum aleuticum
Vittaria lineata
Vittaria appalachiana
Lonchitis hirsuta
Lindsaea linearis
Lindsaea microphylla
Cyatheales
Cyathea spinulosa
Thyrsopteris elegans
Culcita macrocarpa
Plagiogyria japonica
Salviniales
Pilularia globulifera
Azolla cf. caroliniana
Schizaeales
Lygodium japonicum
Anemia tomentosa
Gleicheniales
Dipteris conjugata
Hymenophyllales
Hymenophyllum bivalve
Osmundales
Osmundastrum cinnamomeum
Osmunda javanica
Marattiidae
Marattia attenuata
Danaea nodosa
Ophioglossidae
Psilotum nudum
Tmesipteris parva
Ophioglossum vulgatum
Ophioglossum petiolatum
Botrypus virginianus
Sceptridium dissectum
Botrychium lunaria
Equisetidae
Equisetum diffusum
Equisetum hymale
Isoetes tegetiformans
Selaginella apoda
Selaginella lepidophylla
Lycopodium deuterodensum
Pseudolycopodiella caroliniana
0.61
0.97
0.99
0.98
0.46
3.0
Polypodiidae (Leptosporangiate)
Polypodiospida
Lycopodiopsida